

FRAGMENTATION AND ENERGY CONSERVATION
IN THE EIKONAL-REGGE MODEL*

Shau-Jin Chang†

Department of Physics
University of Illinois, Urbana, Illinois 61801

Tung-Mow Yan††

Stanford Linear Accelerator Center
Stanford University, Stanford, California 94305

ABSTRACT

We have studied the effect of fragmentation and energy conservation in the Eikonal-Regge model. A generalized eikonal representation involving multi-impact-parameters is given for the elastic and inelastic amplitudes when fragmentation takes place. The generalized eikonal function depends on more than one impact parameter which describes a many-body potential. In the strong absorption model and at high energy, however, the elastic amplitude can be approximated by a single impact parameter representation with an effective eikonal function. As a result of the fragmentation, we find that although σ_E and σ_T still increase as $\ln^2 s$, their ratio is no longer 1/2. Instead, it is the sum of the elastic and diffractive cross sections which remains to be one half of the total cross section. To enforce the energy conservation, we propose a thermodynamic approach by introducing an impact-parameter-dependent temperature. Using well-known thermodynamics relations, we obtain various corrections to the naive Eikonal-Regge model predictions due to energy conservation. Experimental consequences are discussed.

*Work supported in part by the U. S. Atomic Energy Commission and in part by the National Science Foundation under Grant No. NSF GP40908X.

†Alfred P. Sloan Foundation Research Fellow, 1972-1974.

††On leave of absence from Cornell University, Ithaca, New York 14850.

I. INTRODUCTION

The eikonal model¹ for high energy scattering of hadrons offers a semi-classical picture for a very complicated process. A most striking characteristics of high energy hadron collisions is the fact that the number distributions in phase space are very different in transverse and longitudinal momentum axes: they are rather limited in the former but apparently not in the latter. The impact parameter representation in the eikonal model is ideal for describing this disparate situation. It nicely separates the transverse degrees of freedom from the dynamics in the longitudinal space.

The main features of the eikonal approach are that, on the one hand, the s-channel unitarity is automatically enforced, and on the other, it can incorporate any energy dependence of the total cross sections consistent with unitarity by a proper choice of the eikonal function. This is in distinction with the conventional Regge approach in which the Pomeron is assumed to be a simple pole. The upper bound for the total cross sections in this case is a constant asymptotically. If the rise in the pp total cross section² observed in recent ISR experiments continues to hold in the future, the simple Regge pole approach must be abandoned. In that case the eikonal model may be a simple alternative to organize the data. Assuming this possibility to exist, we will reexamine and explore further certain aspects in an eikonal model with rising total cross sections.

The eikonal approximation has been studied most thoroughly for the elastic amplitude at high energies and small momentum transfers both in the ϕ^3 theory³⁻⁹ and the massive vector gluon model.¹⁰⁻¹³ The two incident particles are assumed to retain most of their energies throughout the collision. The production processes under the same assumption have also been studied.^{6, 14} Although the presumption of a negligibly small energy loss in the two incident particles does not lead to

any apparent difficulties in the study of the elastic amplitude, this assumption has to be supplemented by a self-consistent procedure in the earlier calculation⁶ of one particle inclusive cross section, number distribution and multiplicities. Otherwise, energy conservation will not be respected.

The purpose of this paper is three-fold.¹⁵ First of all, we will include the fragmentation of the target and the projectile, so that the energy of the initial particles is shared by groups of particles. Secondly, in addition to the repeated exchange of a connected piece between one fragment of the target and another of the projectile, we will also consider the exchange of a connected piece between one group of target fragments and another of projectile fragments. The latter type of exchanges generates energy dependent many-body potentials between target fragments and projectile fragments. Thirdly, we will improve the treatment of energy conservation constraint in the eikonal approach; especially in multiparticle production.

We will show that a generalized eikonal representation can be established for the elastic as well as inelastic amplitudes when both the fragmentation effects and many-body potentials are taken into account. A particularly important result is that when the Froissart bound is saturated, the ratio of the elastic to the total cross section is no longer $1/2$; rather, it is the sum of the elastic and diffractive cross sections which is one half of the total cross section. Another important consequence is the existence of a gap on the rapidity axis between pionization and fragmentation region. This is due to the large multiplicity (proportional to a positive power of the energy) predicted by the model. We must emphasize in the very beginning that although the recent data² show a significant rise in the pp total cross section with energy, and they also suggest a faster than logarithmic

increase of the multiplicity with energy; it remains to be seen whether the predicted ratio of the total to the sum of the elastic and diffractive cross section, and the existence of a rapidity gap will be substantiated by future experiments.

II. THE MODEL

In this paper it will be assumed that only scalar particles are involved in the scattering process. We will study certain class of Feynman graphs in a ϕ^3 theory under specific kinematic conditions appropriate to the eikonal approach. These kinematic conditions will be described more precisely later. We wish to emphasize that it is not our intention to study the asymptotic behavior of the complete theory. We will restrict our discussion to the case where the exchanged connected part is the t-channel ladder, and the momentum flowing into and out of it is in the pionization region. Such an exchanged part exhibits the well-known asymptotic Regge behavior. It will be further assumed that the input Regge intercept $\alpha(0)$ exceeds unity so that the total cross section saturates the Froissart bound. We will refer to such a model as the strong absorption model.

A. Eikonal-Regge Model Without Fragmentation

The model based on the above assumptions plus the additional constraint that the fragmentation is excluded has been studied in Ref. (6). As we shall see, this simplified model contains many important features as in the more complete theory and is much easier to handle. Hence, we shall use this model again in Section III to introduce some useful thermodynamics concepts. The main results in this simplified model for the elastic amplitude and cross sections can be summarized by:

- (1) The elastic amplitude is given by a simple eikonal form

$$T_E = -2is \int d^2b e^{-i\vec{k} \cdot \vec{b}} (1 - e^{-A(s,b)}) \quad (2.1)$$

The eikonal function $A(s, b)$ is assumed to be purely absorptive and given by⁶

$$A(s, b) = \frac{1}{2s} \int \frac{d^2k}{(2\pi)^2} e^{i\vec{k} \cdot \vec{b}} \beta(k) \left(\frac{s}{\mu^2}\right)^{\alpha(k^2)}$$

$$\cong \frac{\beta(0)}{8\pi c\mu^2 \ln \frac{s}{\mu^2}} \left(\frac{s}{\mu^2}\right)^{\alpha(0)-1} e^{-\frac{b^2}{4c \ln s/\mu^2}} \quad (2.2)$$

where $\alpha(k^2)$ and $\beta(k^2)$ are the trajectory function and the residue function respectively, which appear in the ladder amplitude

$$T_L = -i\beta(k^2) \left(\frac{s}{\mu^2}\right)^{\alpha(k^2)}, \quad \alpha(0) > 1 \quad (2.3)$$

(2) The total, the elastic and the inelastic cross sections are given by

$$\sigma_T = -\frac{1}{s} \text{Im } T_E(k^2=0) = 2 \int d^2b (1 - e^{-A(s, b)}) \quad (2.4)$$

$$\sigma_E = \int d^2b (1 - e^{-A(s, b)})^2 \quad (2.5)$$

$$\sigma_I = \sum_{N=1}^{\infty} \sigma_N$$

$$= \int d^2b (1 - e^{-2A(s, b)}) \quad (2.6)$$

$$\sigma_E + \sigma_I = \sigma_T \quad (2.7)$$

where

$$\sigma_N = \int d^2b e^{-2A(s, b)} \frac{(2A)^N}{N!} \quad (2.8)$$

is the inelastic cross section due to opening of N ladders.

We wish to emphasize that the relation of $A(s, b)$ with T_L as in (2.1) and (2.2) is only tentative. The power dependence on s in $A(s, b)$ requires modification in the strong absorption model in order to be consistent with energy conservation.

This point will be discussed in great detail later. However, the modification will not alter the basic structure of the amplitudes. In this section we will therefore continue to employ the standard eikonal approximation in order to arrive efficiently at the general structure. The necessary refinements will be deferred to next section. The readers are referred to Ref. (6) for details of the earlier work.

B. Eikonal Model with Fragmentation

Our aim in this section is to derive a generalized eikonal representation for the elastic and inelastic amplitudes when the fragmentation and many-body potentials are taken into account. Fragmentation effects have been considered previously in simple cases^{10, 13} such as in the electron-photon scattering and photon-photon scattering via multiphoton exchanges. They have also been discussed recently by Skard and Falco,¹⁶ and Blankenbecler et al.¹ Our investigation is a generalization of the earlier work.

Consider the scattering in the center-of-mass system. We are interested in the high energy behavior of the type of Feynman graphs depicted in Fig. 1 and Fig. 2 contributing to the elastic and inelastic amplitudes, respectively. The lines labelled $a_1 \dots a_n$ ($b_1 \dots b_m$) represent the fragments of particle a (particle b). All the other particles in the graphs are in the pionization region. A particle is said to be in the fragmentation region if its longitudinal momentum p_3 satisfies

$$\epsilon p < |p_3| < p \equiv |\vec{p}| = \frac{1}{2} \sqrt{s}, \quad (0 < \epsilon \ll 1) \quad (2.9)$$

where ϵ is small but s -independent; otherwise, it is in the pionization region.

The momentum \vec{p} is related to the initial momenta \vec{p}_a and \vec{p}_b by

$$\vec{p}_a = -\vec{p}_b = \vec{p}, \quad (2.10)$$

and lies in the z-direction. For the elastic amplitude, the final particles momenta are

$$\vec{p}'_a = -\vec{p}'_b = \vec{p} - \vec{k} \quad , \quad \vec{k} = (k_1, k_2) \quad . \quad (2.11)$$

We will calculate first the graphs of Fig. 3 in which particle a dissociates into two particles and particle b retains its identity. Let $T_n^{(2)}$ denote the contribution to T_E from exchange of n such ladders in all possible permutations. We now express $T_n^{(2)}$ as products of various subamplitudes with simple physical interpretation,

$$\begin{aligned} T_n^{(2)}(p'_a) &= i \int \frac{d^4 p_1}{(2\pi)^4} \frac{d^4 p'_1}{(2\pi)^4} \prod_i \left[\frac{d^4 k_i}{(2\pi)^4} \frac{d^4 \ell_i}{(2\pi)^4} \frac{d^4 q_{2i-1}}{(2\pi)^4} \frac{d^4 q_{2i}}{(2\pi)^4} \right] \\ &\times (2\pi)^4 \delta^4(\Sigma k_i + p_1 - p'_1) (2\pi)^4 \delta^4(\Sigma \ell_i + p_2 - p'_2) \\ &\times w(p_1, p_2) w(p'_1, p'_2) D_1^{-1} D_2^{-1} D_b^{-1} \\ &\times \frac{1}{n!} \prod_{i=1}^n \left[B(k_i, \ell_i; q_{2i-1}, q_{2i}) (2\pi)^4 \delta(k_i + \ell_i - q_{2i-1} - q_{2i}) \right] \end{aligned} \quad (2.12)$$

where

$$p_2 = p_a - p_1 \quad , \quad p'_2 = p'_a - p_1 \quad (2.13)$$

We shall define and simplify these subamplitudes separately:

(1) The amplitude $w(p_1, p_2)$ describes the dissociation of particle a into particles 1 and 2,

$$\begin{aligned} w(p_1, p_2) &= ig^+ \frac{i}{p_1^- - \mu^2 + i\epsilon} \frac{i}{p_2^- - \mu^2 + i\epsilon} \\ &= \frac{-ig^+}{p_1^+ p_2^+} \frac{1}{p_1^- - E^-(p_1) + i\epsilon} \frac{1}{p_2^- - E^-(p_2) + i\epsilon} \\ &= \frac{ig^+}{p_1^+ p_2^+} \frac{1}{E^-(p_1) + E^-(p_2) - p_a^-} \left[\frac{1}{p_1^- - E^-(p_1) + i\epsilon} + \frac{1}{p_2^- - E^-(p_2) + i\epsilon} \right] \end{aligned} \quad (2.14)$$

where

$$p_i^\pm \equiv p_i^0 \pm p_i^3, \quad (i = 1, 2) \quad (2.15)$$

$$E^-(p) \equiv \frac{\vec{p}_\perp^2 + \mu^2}{p^+} \quad (2.16)$$

In the fragmentation region, the fractional longitudinal momentum x defined by

$$p_1^+ = xp_a^+ = x\sqrt{s}, \quad 0 < x < 1, \quad (2.17)$$

is finite. Then, we find that $E^-(p_1)$ and $E^-(p_2)$ are of $O(1/\sqrt{s})$ and $p_2^- = -p_1^- + O(1/\sqrt{s})$. Ignoring terms of $O(1/\sqrt{s})$, we have

$$\begin{aligned} \frac{1}{p_1^- - E^-(p_1) + i\epsilon} + \frac{1}{p_2^- - E^-(p_2) + i\epsilon} &= \frac{1}{p_1^- + i\epsilon} + \frac{1}{-p_1^- + i\epsilon} \\ &= -2\pi i \delta(p_1^-) \end{aligned} \quad (2.18)$$

and, consequently

$$\begin{aligned} w(p_1, p_2) &= \frac{g}{p_1^+ p_2^+} \frac{1}{E^-(p_1) + E^-(p_2) - p_a^-} (2\pi) \delta(p_1^-) \\ &= \frac{p_a^+}{p_1^+ p_2^+} \psi(p_1, p_2) (2\pi) \delta(p_1^-), \end{aligned} \quad (2.19)$$

where $\psi(p_1, p_2)$ is the infinite momentum wave function describing the dissociation,

$$\begin{aligned} \psi(p_1, p_2) &\equiv \frac{g}{p_a^+ [E^-(p_1) + E^-(p_2) - p_a^-]} \\ &= \frac{g}{\frac{\vec{p}_1^2 + \mu^2}{x} + \frac{\vec{p}_2^2 + \mu^2}{1-x} - (\vec{p}^2 + \mu^2)} \\ &= \frac{x(1-x)g}{\vec{p}_{12}^2 + (1-x+x^2)\mu^2}, \end{aligned} \quad (2.20)$$

with

$$\vec{p}_{12} = (1-x) \vec{p}_1 - x \vec{p}_2 \quad (2.21)$$

being the relative momentum.

Similarly, the amplitude $w'(p'_1, p'_2)$ describes the recombination of particles 1' and 2' into a', and is given by

$$\begin{aligned} w'(p'_1, p'_2) &= ig \frac{i}{p_1'^2 - \mu^2 + i\epsilon} \frac{i}{p_2'^2 - \mu^2 + i\epsilon} \\ &= \frac{p_a'^+}{p_1'^+ p_2'^+} \psi(p'_1, p'_2) 2\pi \delta(p_1'^-) \quad . \end{aligned} \quad (2.22)$$

The fact that $\psi(p_1, p_2)$ and $\psi(p'_1, p'_2)$ depend only on their relative momenta is extremely important in later interpretation.

(2) The denominator factors D_1^{-1} , D_2^{-1} and D_b^{-1} describe the products of the propagators along particles 1, 2 and b respectively. A summation over all possible permutations of the exchange particles along the fragments 1, 2 and b is understood in the definition of these D^{-1} 's. When k, ℓ, q and r are in the pionization region, i. e., when k^\pm, ℓ^\pm, q^\pm , and $r^\pm \ll \sqrt{s}$, the (D^{-1}) 's can be simplified using the well-known identities¹⁰:

$$\begin{aligned} \delta(\Sigma k_i^-) D_1^{-1} &\equiv \delta(\Sigma k_i^-) \sum_{\text{all perm}} \left[\frac{i}{(p_1+k_1)^2 - \mu^2 + i\epsilon} \frac{i}{(p_1+k_1+k_2)^2 - \mu^2 + i\epsilon} \times \dots \times \right. \\ &\quad \left. \times \frac{i}{(p_1+k_1+\dots+k_n)^2 - \mu^2 + i\epsilon} \right] \\ &= \frac{1}{(p_1^+)^{n-1}} (2\pi)^{n-1} \delta(k_1^-) \delta(k_2^-) \times \dots \times \delta(k_n^-) \quad , \end{aligned} \quad (2.23)$$

$$\begin{aligned}
\delta(\Sigma \ell_j^-) D_2^{-1} &\equiv \delta(\Sigma \ell_j^-) \sum_{\text{all perm}} \left[\frac{i}{(p_2 + \ell_1)^2 - \mu^2 + i\epsilon} \times \dots \times \frac{i}{(p_2 + \ell_1 + \dots + \ell_n)^2 - \mu^2 + i\epsilon} \right] \\
&= \frac{1}{(p_2^+)^{n-2}} (2\pi)^{n-1} \delta(\ell_1^-) \delta(\ell_2^-) \times \dots \times \delta(\ell_n^-) \quad , \quad (2.24)
\end{aligned}$$

and

$$\begin{aligned}
\delta(\Sigma q_i^+) D_b^{-1} &\equiv \delta(\Sigma q^+) \sum_{\text{all perm}} \left[\frac{i}{(p_b - q_1)^2 - \mu^2 + i\epsilon} \times \dots \times \frac{i}{(p_b - q_1 - \dots - q_{2n})^2 - \mu^2 + i\epsilon} \right] \\
&= \frac{(2\pi)^{2n-1}}{(p_b^-)^{2n-1}} \delta(q_1^+) \times \dots \times \delta(q_{2n}^+) \quad (2.25)
\end{aligned}$$

(3) The function $B(k, \ell, q_1, q_2)$ denotes the amplitude of a blob in Fig. 3, including the four vertices $(ig)^4$, and the four propagators

$$\frac{i}{k^2 - \mu^2 + i\epsilon} \times \frac{i}{\ell^2 - \mu^2 + i\epsilon} \times \frac{i}{q_1^2 - \mu^2 + i\epsilon} \times \frac{i}{q_2^2 - \mu^2 + i\epsilon} \quad .$$

If we identify B as the sum of ladder graphs, then B behaves like a Regge pole at large s .

(4) A combinational factor $\frac{1}{n!}$ associates with the n (identical) blobs.

(5) The δ -functions appearing in $T_n^{(2)}$ can be integrated readily after we introduce the light front variables (q^\pm, \vec{q}) , and rewrite the phase space d^4q and the δ -function $\delta^4(q)$ in the form

$$d^4q = \frac{1}{2} dq^+ dq^- d^2q \quad (2.26)$$

$$\delta^4(q) = 2 \delta(q^+) \delta(q^-) \delta^2(\vec{q}) \quad . \quad (2.27)$$

In particular, we have

$$\begin{aligned}
&\delta^4(\Sigma k_i + p_1 - p_1') \delta^4(\Sigma \ell_j + p_2 - p_2') \\
&= 4 \delta(\Sigma k_i^+ + p_1^+ - p_1'^+) \delta^2(\Sigma \vec{k}_i + \vec{p}_1 - \vec{p}_1') \delta^2(\Sigma \vec{\ell}_j + \vec{p}_2 - \vec{p}_2') \\
&\quad \times \delta(\Sigma k_i^- + \Sigma \ell_j^-) \delta(\Sigma k_i^-) \delta(\Sigma \ell_j^-) \quad (2.28)
\end{aligned}$$

where we have ignored terms of $O(1/\sqrt{s})$, such as $p_a^+ - p_a'^+$, p_1^- , and $p_1'^-$. The last three δ -functions in (2.28) will be used to convert (D^{-1}) 's into products of δ -functions as given in (2.23) - (2.25).

Putting parts (1) - (5) together and carrying out the integrations, we obtain

$$\begin{aligned}
T_n^{(2)}(p_a') &= i \int \frac{dp_1^+ dp_1^- d^2 p_1}{2(2\pi)^4} \frac{dp_1'^+ dp_1'^- d^2 p_1'}{2(2\pi)^4} \prod_{i=1}^n \left[\frac{dk_i^+ dk_i^- d^2 k_i}{2(2\pi)^4} \right. \\
&\quad \times \left. \frac{d\ell_i^+ d\ell_i^- d^2 \ell_i}{2(2\pi)^4} \frac{dq_{2i}^+ dq_{2i}^- d^2 q_{2i}}{2(2\pi)^4} \right] 4(2\pi)^5 \delta(\Sigma k_i^+ + p_1^+ - p_1'^+) \\
&\quad \times \delta^2(\Sigma \vec{k}_i + \vec{p}_1 - \vec{p}_1') \delta^2(\Sigma \vec{\ell}_i + \vec{p}_2 - \vec{p}_2') \frac{p_a^+}{p_1^+ p_2^+} \psi(p_1, p_2) 2\pi \delta(p_1^-) \\
&\quad \times \frac{p_a'^+}{p_1'^+ p_2'^+} \psi(p_1', p_2') 2\pi \delta(p_1'^-) \frac{1}{n!} p_1^+ p_2^+ p_b^- \\
&\quad \times \prod_{i=1}^n \left[\frac{(2\pi)^4 \delta(k_i^-) \delta(\ell_i^-) \delta(q_{2i-1}^+) \delta(q_{2i}^+)}{p_1^+ p_2^+ (p_b^-)^2} B(k_i, \ell_i, q_{2i-1}, q_{2i}) \right] \\
&= 2is \int \frac{dx}{4\pi x(1-x)} \frac{d^2 p_1}{(2\pi)^2} \frac{d^2 p_1'}{(2\pi)^2} \psi(p_1, p_2) \psi(p_1', p_2') \\
&\quad \times (2\pi)^2 \delta(\Sigma \vec{k}_i + \vec{p}_1 - \vec{p}_1') (2\pi)^2 \delta(\Sigma \vec{\ell}_i + \vec{p}_2 - \vec{p}_2') \\
&\quad \times \frac{1}{n!} \prod_{i=1}^n \left[F(s_1, s_2, \vec{k}_i, \vec{\ell}_i) \frac{d^2 k_i}{(2\pi)^2} \frac{d^2 \ell_i}{(2\pi)^2} \right] \tag{2.29}
\end{aligned}$$

where

$$\begin{aligned}
p_1^+ &\cong p_1'^+ = xp_a^+ , \\
F(s_1, s_2; \vec{k}, \vec{\ell}) &\equiv \frac{1}{2s_1 s_2} \int \frac{dk^+}{4\pi} \int \frac{dq_1^-}{4\pi} \frac{d^2 q_1}{(2\pi)^2} \frac{d^2 q_2}{(2\pi)^2} (2\pi)^2 \delta(\vec{q}_1 + \vec{q}_2 - \vec{k} - \vec{\ell}) \\
&\quad \times B(k, \ell, q_1, q_2) \Big|_{\substack{k^- = \ell^- = 0 \\ q_1^+ = 0}} , \tag{2.31}
\end{aligned}$$

and

$$\begin{aligned}
s_1 &\equiv (p_1^+ p_b^-)^2 \cong p_1^+ p_b^- = xs , \\
s_2 &\equiv (p_2^+ p_b^-)^2 \cong p_2^+ p_b^- = (1-x)s . \tag{2.32}
\end{aligned}$$

The result is particularly transparent in the impact parameter representation,

$$\begin{aligned}
\tilde{T}_n^{(2)}(b) &\equiv \int \frac{d^2 p'_a}{(2\pi)^2} e^{i(\vec{p}'_a - \vec{p}_a) \cdot \vec{b}} T_n^{(2)}(p'_a) \\
&= 2is \int \frac{dx}{4\pi x(1-x)} \int d^2 b_{12} |\Psi(b_{12})|^2 \\
&\quad \times \frac{1}{n!} \left[-a(s_1, s_2, b_1, b_2) \right]^n , \tag{2.33}
\end{aligned}$$

where

$$\begin{aligned}
\Psi(b_{12}) &\equiv \int \frac{d^2 p_{12}}{(2\pi)^2} e^{i\vec{p}_{12} \cdot \vec{b}_{12}} \psi(p_{12}) \\
&= \frac{x(1-x)g}{2\pi} K_0(\sqrt{1-x+x^2} \mu b_{12}) \tag{2.34}
\end{aligned}$$

is the coordinate space wave function,

$$\begin{aligned}
a(s_1, s_2, b_1, b_2) & (= i \chi(s_1, s_2, b_1, b_2)) \\
& \equiv - \int \frac{d^2 k}{(2\pi)^2} \frac{d^2 \ell}{(2\pi)^2} e^{i \vec{k} \cdot \vec{b}_1 + i \vec{\ell} \cdot \vec{b}_2} F(s_1, s_2, k, \ell)
\end{aligned} \tag{2.35}$$

is the (3-body) eikonal potential, and

$$\vec{b}_1 = \vec{b} + (1-x) \vec{b}_{12}, \quad \vec{b}_2 = \vec{b} - x \vec{b}_{12} \tag{2.36}$$

are the impact parameters of the individual fragments. Summing over all n , we obtain

$$\tilde{T}_E^{(2)}(b) = 2is \int \frac{dx}{4\pi x(1-x)} \int d^2 b_{12} |\Psi(b_{12})|^2 \left(e^{-a(s_1, s_2, b_1, b_2)} - 1 \right) \tag{2.37}$$

and consequently,

$$\begin{aligned}
T_E^{(2)}(p'_a) & = 2is \int d^2 b_1 d^2 b_2 e^{-i(\vec{p}'_a - \vec{p}_a) \cdot \vec{b}} \int \frac{dx}{4\pi x(1-x)} \\
& \quad \times |\Psi(b_{12})|^2 \left[e^{-a(s_1, s_2, b_1, b_2)} - 1 \right]
\end{aligned} \tag{2.38}$$

where

$$\vec{b} = x \vec{b}_1 + (1-x) \vec{b}_2, \quad \vec{b}_{12} = \vec{b}_1 - \vec{b}_2. \tag{2.39}$$

Equations (2.37) and (2.38) can be generalized in several ways. If the usual two-body potentials are included (see Fig. 4), we only have to make the replacement in the eikonal function

$$\begin{aligned}
a(s_1, s_2, b_1, b_2) & \rightarrow A(s_1, s_2, b_1, b_2) = a(s_1, b_1) + a(s_2, b_2) \\
& \quad + a(s_1, s_2, b_1, b_2)
\end{aligned} \tag{2.40}$$

where $a(s_1, b_1)$ [$a(s_2, b_2)$] corresponds to the exchange of two-body potentials between particle 1 [particle 2] and particle b, and is given by

$$\begin{aligned}
a(s_1, b_1) = & -\frac{1}{4s_1} \int \frac{dk_1^+}{4\pi} \frac{dq_1^-}{4\pi} \frac{d^2k_1}{(2\pi)^2} \frac{d^2k_2}{(2\pi)^2} \frac{d^2q_1}{(2\pi)^2} \frac{d^2q_2}{(2\pi)^2} \\
& \times (2\pi)^2 \delta(\vec{q}_1 + \vec{q}_2 - \vec{k}_1 - \vec{k}_2) e^{i(\vec{k}_1 + \vec{k}_2) \cdot \vec{b}_1} \\
& \times B(k_1, k_2, q_1, q_2) \Big|_{k_i^- = 0, q_i^+ = 0} .
\end{aligned} \tag{2.41}$$

For the same blob amplitude (here ladder) B, there is a relation between $a(s, b)$ and $a(s_1, s_2, b_1, b_2)$

$$a(s_1, s_2, b, b) = 2a(\sqrt{s_1 s_2}, b) . \tag{2.42}$$

Suppose now that particle a dissociates into more than two fragments, say three, as in Fig. 5. These graphs can be calculated similarly. Only the fragmentation parts need some comments. In the following, we only present the results. The detailed analysis leading to these results will be published in a separate paper.

The elastic amplitude for the process described in Fig. 5 can be written as

$$\begin{aligned}
T_E^{(3)}(p_a') = & 2is \int \frac{dx_1}{4\pi x_1} \frac{dx_2}{4\pi x_2} \frac{dx_3}{4\pi x_3} 4\pi \delta(x_1 + x_2 + x_3 - 1) d^2b_1 d^2b_2 d^2b_3 \\
& \times |\psi(x_i, \vec{b}_1 - \vec{b}_2, \vec{b}_1 - \vec{b}_3)|^2 e^{-i(\vec{p}_a - \vec{p}_a') \cdot \vec{b}} \left[e^{-A(\{s_i\}, \{b_i\})} - 1 \right]
\end{aligned} \tag{2.43}$$

where ψ is the three-particle wave function,

$$\vec{b} \equiv x_1 \vec{b}_1 + x_2 \vec{b}_2 + x_3 \vec{b}_3 , \tag{2.44}$$

and

$$\begin{aligned}
A(\{s_i\}, \{b_i\}) = & a(s_1, b_1) + a(s_2, b_2) + a(s_3, b_3) \\
& + a(s_1, s_2, b_1, b_2) + a(s_2, s_3, b_2, b_3) + a(s_3, s_1, b_3, b_1)
\end{aligned} \tag{2.45}$$

When more general exchanges are included, the potential $A(\{s_i\}, \{b_i\})$ should contain true four-body potentials as well.

The fragmentation of particle b can also be easily included. For example, the result for $a \rightarrow a_1 + a_2$, and $b \rightarrow b_1 + b_2$ (Fig. 6) is ($p_{ai}^+ = x_i p_a^+$, $p_{bi}^- = y_i p_b^-$)

$$\begin{aligned}
T_E^{(2,2)} = & -2is \int \frac{dx_1}{4\pi x_1} \frac{dx_2}{4\pi x_2} 4\pi \delta(x_1+x_2-1) d^2b_1 d^2b_2 \delta(x_1\vec{b}_1 + x_2\vec{b}_2 - \vec{b}) \\
& \times \frac{dy_1}{4\pi y_1} \frac{dy_2}{4\pi y_2} 4\pi \delta(y_1+y_2-1) d^2c_1 d^2c_2 \delta(y_1\vec{c}_1 + y_2\vec{c}_2) \\
& \times |\psi(x, b_{12})|^2 |\psi(y, c_{12})|^2 \int d^2b e^{-i(\vec{p}_a^+ - \vec{p}_a^-) \cdot \vec{b}} \\
& \times \left[1 - e^{-A(\{s_i\}, \{\vec{b}_i, \vec{c}_j\})} \right] \tag{2.46}
\end{aligned}$$

where \vec{b}_1 , \vec{b}_2 , and \vec{c}_1 , \vec{c}_2 describe the positions of the fragments relative to c. m. of particle b, and $\psi(x, b)$ and $\psi(y, c)$ are their respective wave functions. As a result of momentum conservation, the potential $A(\{s_i\}, \{\vec{b}_i, \vec{c}_j\})$ depends on the impact parameter \vec{b} and the coordinates \vec{b}_i and \vec{c}_j only through the differences $\vec{b}_i - \vec{c}_j$ ($i, j = 1, \text{ or } 2$).

In the special case of the exchange of a four-body potential as depicted in Fig. 7, the eikonal function A in (2.46) is given by

$$\begin{aligned}
a(\{s\}, b_1, b_2, c_1, c_2) = & -\frac{1}{x(1-x)y(1-y)s^2} \int \frac{dk_1^+}{4\pi} \frac{dq_1^-}{4\pi} \frac{d^2k_1}{(2\pi)^2} \\
& \times \frac{d^2k_2}{(2\pi)^2} \frac{d^2q_1}{(2\pi)^2} \frac{d^2q_2}{(2\pi)^2} (2\pi)^2 \delta^2(\vec{k}_1 + \vec{k}_2 - \vec{q}_1 - \vec{q}_2) \\
& \times e^{i\vec{k}_1 \cdot \vec{b}_1 + i\vec{k}_2 \cdot \vec{b}_2 - i\vec{q}_1 \cdot \vec{c}_1 - i\vec{q}_2 \cdot \vec{c}_2} B(k_1, k_2, q_1, q_2) \Big|_{\substack{k_1^- = 0 \\ q_1^+ = 0}} \tag{2.47}
\end{aligned}$$

It is easy to see that $a(\{s\}, b_1, b_2; c_1, c_2)$ is a function of $x(1-x)$ $y(1-y)$ s and $b_i - c_j$ ($i, j = 1, 2$) only. When the previously considered two-body and three-body potentials are included, they contribute additively to the eikonal function.

The result (2.46) generalizes easily to the case in which particle a and particle b fragment into more than two particles.

C. Production Processes with Fragmentations

The inelastic amplitudes can be calculated by similar technique.¹⁷ Only fragmentation of particle a will be considered. To be specific, let's consider the high energy limit of graphs in Fig. 8. Summing over graphs with all permutations of the vertices attached to the three energetic lines and making use of results in Section II.B, we obtain the simplified amplitude

$$\begin{aligned}
T(N_1, N_2, N_{12}, \dots) = 2 \text{ is } & \int d^2 b_1 d^2 b_2 e^{-i(\vec{p}_1 - x \vec{p}_a) \cdot \vec{b}_1 - i(\vec{p}_2 - (1-x) \vec{p}_a) \cdot \vec{b}_2} \\
& \times \Psi(x, b_{12}) \frac{1}{N_1!} [-a(s_1, b_1)]^{-N_1} \frac{1}{N_2!} [-a(s_2, b_2)]^{-N_2} \frac{1}{N_{12}!} [-a(s_1, s_2, b_1, b_2)]^{N_{12}} \\
& \times \prod_k \left(-\frac{i}{2xs} \tilde{M}_k(b_1) \right) \prod_\ell \left(-\frac{i}{2(1-x)s} \tilde{M}_\ell(b_2) \right) . \quad (2.48)
\end{aligned}$$

Summing over all absorption corrections we obtain the eikonal representation

$$\begin{aligned}
T_I(s, p_1', p_2', \{k\}) = 2 \text{ is } & \int d^2 b_1 d^2 b_2 e^{-i(\vec{p}_1 - x \vec{p}_a) \cdot \vec{b}_1 - i(\vec{p}_2 - (1-x) \vec{p}_a) \cdot \vec{b}_2} \\
& \times \Psi(x, b_{12}) e^{-A(\{s_i\}, b_1, b_2)} \prod_k \left(-\frac{i}{2xs} \tilde{M}_k(b_1) \right) \prod_\ell \left(-\frac{i}{2(1-x)s} \tilde{M}_\ell(b_2) \right) \quad (2.49)
\end{aligned}$$

where $A(\{s_i\}, b_1, b_2)$ is given by (2.40) and $M_k(b_1)$ is the Fourier transform of the multiperipheral amplitude

$$M_k(q) = i (ig)^{n+2} \frac{i}{q^2 - \mu^2 + i\epsilon} \times \dots \times \frac{i}{(q+k_1+\dots+k_n)^2 - \mu^2 + i\epsilon} \quad (2.50)$$

with the momentum labels $\{k_1, k_2, \dots, k_n\}$ suppressed.

A scattering process is defined to be diffractive if only the fragmentation particles are produced without being accompanied by any pionization particle. The amplitude for a diffractive process $a \rightarrow a_1 + a_2$ is

$$\begin{aligned} T_D^{(2)} = & -e i s \int d^2 b_1 d^2 b_2 e^{-i(\vec{p}'_1 - x\vec{p}'_a) \cdot \vec{b}_1 - i(\vec{p}'_2 - (1-x)\vec{p}'_a) \cdot \vec{b}_2} \\ & \times \Psi(x, b_{12}) \left(1 - e^{-A(s_1, s_2, b_1, b_2)} \right) . \end{aligned} \quad (2.51)$$

From the amplitude given by (2.49) and (2.51) we can calculate the various cross sections. For example, the differential diffractive cross section from (2.51) is

$$\begin{aligned} d\sigma_D^{(2)} = & \frac{1}{2} |T_D^{(2)}|^2 \frac{1}{2E_a 2E_b} \frac{d^3 p'_1}{2E'_1 (2\pi)^3} \frac{d^3 p'_2}{2E'_2 (2\pi)^3} \frac{d^3 p'_b}{2E'_b (2\pi)^3} \\ & \times (2\pi)^4 \delta^4(p'_1 + p'_2 + p'_b - p_a - p_b) \\ = & \frac{1}{4s^2} |T_D^{(2)}(p'_1, p'_2)|^2 \frac{dx}{4\pi x(1-x)} \frac{d^2 p'_1}{(2\pi)^2} \frac{d^2 p'_2}{(2\pi)^2} . \end{aligned} \quad (2.52)$$

The p'_1, p'_2 integrations can be carried out trivially, and we obtain

$$\sigma_D^{(2)} = \int d^2 b_1 d^2 b_2 \int \frac{dx}{4\pi x(1-x)} |\Psi(x, b_{12})|^2 \left(1 - e^{-A(s_1, s_2, b_1, b_2)} \right)^2 \quad (2.53)$$

Similarly, from (2.49) we get

$$\sigma_I^{(2)} = \int d^2 b_1 d^2 b_2 \int \frac{dx}{4\pi x(1-x)} |\Psi(x, b_{12})|^2 \left(1 - e^{-2A(s_1, s_2, b_1, b_2)} \right) \quad (2.54)$$

Thus

$$\begin{aligned}
\sigma_D^{(2)} + \sigma_I^{(2)} &= 2 \int d^2b_1 d^2b_2 \int \frac{dx}{4\pi x(1-x)} |\Psi(x, b_{12})|^2 \left(1 - e^{-A(s_1, s_2, b_1, b_2)}\right) \\
&= -\frac{1}{s} \text{Im } T_E^{(2)}(p_a' - p_a = 0) \\
&= \sigma_T^{(2)}
\end{aligned} \tag{2.55}$$

where $T_E^{(2)}$ is given by (2.38) with the eikonal function (2.40). Equation (2.55) is the optical theorem in this case.

Before we proceed further, we will derive a simplified, single impact parameter representation for various amplitudes and cross sections. We note the relation

$$\begin{aligned}
&2 \left[a(s_1, b_1) + a(s_2, b_2) \pm a(s_1, s_2, b_1, b_2) \right] \\
&= \sum_n \int_{i=1}^n \frac{d^3k_i}{(2\pi)^3 2k_i^0} \left| \frac{1}{2xs} \tilde{M}(b_1, \{k\}) \pm \frac{1}{2(1-x)s} \tilde{M}(b_2, \{k\}) \right|^2 \\
&> 0
\end{aligned} \tag{2.56}$$

which implies

$$a(s_1, b_1) + a(s_2, b_2) \geq a(s_1, s_2, b_1, b_2) \quad . \tag{2.57}$$

Further, since $a(s_1, s_2, b_1, b_2)$ is positive,¹⁸ we finally obtain the inequalities

$$\begin{aligned}
1 - e^{-a(s_1, b_1) - a(s_2, b_2)} &\leq 1 - e^{-a(s_1, b_1) - a(s_2, b_2) - a(s_1, s_2, b_1, b_2)} \\
&\leq 1 - e^{-2[a(s_1, b_1) + a(s_2, b_2)]}
\end{aligned} \tag{2.58}$$

But in the high energy limit, the upper and lower bound approach each other and

$$\begin{aligned}
1 - e^{-A(s_1, s_2, b_1, b_2)} &= 1 - \left[1 - \theta(b_m - b_1)\right] \left[1 - \theta(b_m - b_2)\right] \\
&= \theta(b_m - b_1) + \theta(b_m - b_2) - \theta(b_m - b_1) \theta(b_m - b_2)
\end{aligned} \tag{2.59}$$

where b_m is determined by $a(s_1, b_1)$ or $a(s_2, b_2)$ alone.

In the strong coupling case and at high energy, b_m increases as $\ln s$ and has no x -dependence, while b_{12} ($\equiv b_1 - b_2$) is finite and controlled by the wave function $\Psi(b_{12})$. Hence it is a good approximation to ignore the x and b_{12} -dependence in A and to replace $A(s_1, s_2, b_1, b_2)$ by $A(s, b)$ where $\vec{b} \equiv x\vec{b}_1 + (1-x)\vec{b}_2$ is the impact parameter associated with the center of momentum of particle a. After this replacement, we then arrive at the single impact parameter representation results,

$$T_E^{(2)} = -2is I_2 \int d^2b e^{-i(\vec{p}'_a - \vec{p}_a) \cdot \vec{b}} \left(1 - e^{-A(s, b)}\right) \quad (2.60)$$

$$\sigma_D^{(2)} = I_2 \int d^2b \left(1 - e^{-A(s, b)}\right)^2 \quad (2.61)$$

$$\sigma_I^{(2)} = I_2 \int d^2b \left(1 - e^{-2A(s, b)}\right) \quad (2.62)$$

where the positive constant I_2 is given by

$$I_2 \equiv \int d^2b_{12} \int \frac{dx}{4\pi x(1-x)} |\Psi(x, b_{12})|^2 \quad (2.63)$$

Under this approximation, we obtain from (2.52), (2.59),

$$\sigma_D^{(2)} = \sigma_I^{(2)} = \frac{1}{2} \sigma_T^{(2)} \quad (2.64)$$

The above discussion can be generalized to more complicated situation. In our later discussion we will therefore very frequently ignore the coordinate (such as b_{12}) dependence in the wave functions, and base our discussion on the single impact parameter representation. In this approximation if only the fragmentation of particle a is considered, the contribution to the elastic amplitude from the fragmentation into N particle can be written as

$$T_E^{(N)} = -2is \int d\Gamma_N^{(a)}(1, \dots, N) \int d^2b e^{-i\vec{k} \cdot \vec{b}} \left(1 - e^{-A_N(s, b)}\right) \quad (2.65)$$

and the full elastic amplitude is

$$T_E = \sum_{N=1}^{\infty} T_E^{(N)} . \quad (2.66)$$

In the strong absorption model all the $A_N(s, b)$'s have the same size:

$$1 - e^{-A_N(s, b)} = \theta(b_m - b), \quad (b_m = b_0 \ln s) , \quad (2.67)$$

and we obtain

$$\sigma_T = -\frac{1}{s} \text{Im} T_E = \left(\sum_{N=1}^{\infty} \int dI_N^{(a)} \right) 2\pi b_m^2 , \quad (2.68)$$

$$\sigma_D = \sum_{N=2}^{\infty} \sigma_D^{(N)} = \left(\sum_{N=2}^{\infty} \int dI_N^{(a)} \right) \pi b_m^2 . \quad (2.69)$$

There are two methods from which σ_E can be determined:

- (1) σ_E is identified as the elastic contribution to σ_T , and
- (2) σ_E is obtained directly from T_E through integration.

For a complete theory, these two definitions will lead to identical results. In our theory, since we have not considered all the diagrams contributing to σ_T and T_E , these two approaches may give rise to different answers. As we shall see, if we insist that both methods lead to the same answer, we shall arrive at some very restrictive predictions in σ_E/σ_T .

We will assign $T_E^{(1)}$, the contribution to the elastic amplitude without fragmentation, to be

$$T_E^{(1)} = -2is c^{(a)} \int d^2b e^{-i\vec{k}\cdot\vec{b}} \left(1 - e^{-A(s, b)} \right) \quad (2.70)$$

and the positive constant $c^{(a)}$ ($= \int dI_0^{(a)}$) is chosen to satisfy the unitarity. The elastic cross section σ_E is given by the term on the right-hand side of (2.68) with only elastic intermediate state. This is given by half of the absorptive part

of (2.70), in analogy to (2.54):

$$\sigma_E = c^{(a)} \pi b_m^2 \quad (2.71)$$

From (2.68), (2.69), and (2.71), we conclude that

$$\sigma_E + \sigma_D = \frac{1}{2} \sigma_T \quad (2.72)$$

By method 2, σ_E can also be calculated directly from (2.66). The result is

$$\sigma_E = \left(c^{(a)} + \sum_{N=2}^{\infty} \int dI_N^{(a)} \right)^2 \pi b_m^2 \quad (2.73)$$

Equating the two expressions we find

$$c^{(a)} = \frac{1}{2} [1 - 2z + \sqrt{1 - 4z}] , \quad z = \sum_{N=2}^{\infty} \int dI_N^{(a)} \quad (2.74)$$

where we have chosen the sign of the square root such that $c^{(a)} = 1$ when $z=0$.

Since $c^{(a)}$ must be positive, Eq. (2.74) implies

$$\begin{aligned} 0 < z < \frac{1}{4} , \\ \frac{1}{4} < c^{(a)} < 1 , \end{aligned} \quad (2.75)$$

and consequently,

$$\frac{1}{4} \sigma_T < \sigma_E < \frac{1}{2} \sigma_T \quad (2.76)$$

When the fragmentation of both particles a and b is considered, Eq. (2.72)

remains unchanged but (2.76) now becomes

$$\frac{1}{8} \sigma_T < \sigma_E < \frac{1}{2} \sigma_T \quad (2.77)$$

The result (2.72) has also been obtained by Blankenbecler, Fulco and Sugar¹ in a different model. Its validity appears to be very general. It is interesting that there is also a lower limit on the ratio σ_E/σ_T in our model. It follows from

(2.68) and (2.74) that

$$\sigma_T = \sqrt{c^{(a)}} 2\pi b_m^2 < 2\pi b_m^2 . \quad (2.78)$$

Therefore, the disc is not completely black. Of course, this is why the ratio σ_E/σ_T is less than one-half.

III. ENERGY CONSERVATION CONSTRAINT AND TEMPERATURE SPACE

We now turn to the question of energy conservation in the eikonal approximation. We will first neglect completely the fragmentation events. Their inclusion will be discussed in the next section.

A. The Temperature Space

In ϕ^3 model, the inelastic cross section due to opening of N ladders can be written as (see Eq. (3.11), Ref. 6)

$$d\sigma_N = \int d^2b \cdot e^{-2A(s,b)} \prod_{i=1}^N \sum_{n=1}^{\infty} \left| \frac{1}{2s} \tilde{M}(b, k_1^{(i)}, \dots, k_n^{(i)}) \right|^2 \quad (3.1)$$

where

$$2A(s,b) = \sum_n \int \left| \frac{1}{2s} \tilde{M}(b, k_1, \dots, k_n) \right|^2 \prod_{i=1}^n \frac{d^3k_i}{(2\pi)^3 2\epsilon_i} \quad (3.2)$$

All the momenta $k_j^{(i)}$ belong to particles in the pionization region. The limits of integration of each \vec{k}_i are restricted to

$$\mu \leq \epsilon_i < \eta\sqrt{s} \quad 0 < \eta \ll 1 \quad (3.3)$$

by an order of magnitude estimate. From (3.1) we obtain the integrated cross sections

$$\sigma_N \equiv \int d\sigma_N = \frac{1}{N!} \int d^2b (2A(s,b))^N e^{-2A(s,b)} \quad (3.4)$$

Note that σ_N stands for N "open blob" final states which usually contains more than N final particles. The upper limit given by (3.3) is an over-estimate when the multiplicity grows as a power of s, as in the case of strong absorption. In our earlier work⁶ this difficulty is corrected by a self-consistent argument. Here we propose a more satisfactory solution.

We propose to make the energy conservation constraint explicit by rewriting (3.1) (or 3.4) as

$$\sigma_N = \frac{1}{N!} \int d^2b \frac{\Pi_N(s, b)}{\Pi(s, b)} \quad (3.5)$$

$$\Pi_N(s, b) = \int \prod_{\text{all } i} \frac{d^3k_i}{(2\pi)^3 2\epsilon_i} \prod_{i=1}^N \sum_{n=1}^{\infty} \left| \frac{1}{2s} \tilde{M}(b, k_1^{(i)}, \dots, k_n^{(i)}) \right|^2 \theta\left(E - \sum_{\text{all } \ell} \epsilon_\ell\right) \quad (3.6)$$

and

$$\Pi(s, b) = \sum_{N=0}^{\infty} \frac{1}{N!} \Pi_N(s, b) \quad , \quad \left[\Pi_0 \equiv 1 \right]$$

where $E = \epsilon\sqrt{s}$ is the maximum energy available for producing pionization particles. In our model, ϵ is a small ($0 < \epsilon \ll 1$) but s -independent constant. For the power s -dependence is concerned, it is sufficient to remember that $E \sim \sqrt{s}$.

There are at least three reasons for making such a modification:

- (1) This is the simplest modification which incorporates explicitly the overall energy conservation constraints;
- (2) From the perturbation point of view and for any fixed order n , the introduction of θ -function in (3.5) and (3.6) does not affect the leading logarithmic calculation. The modification becomes important only for large n (say $n \sim s^a$) where the leading logarithmic calculation is no longer reliable; and
- (3) Although the energy conservation constraint destroys the factorizability of the individual ladder amplitudes; the factorizability is regained by making a Laplace transform with respect to E .

After the Laplace transform, we have

$$\begin{aligned}\tilde{\Pi}_N(\tau, b) &= \int_0^\infty dE e^{-\tau E} \Pi_N(s, b) \\ &= \frac{1}{\tau} [2\tilde{A}(\tau, b)]^N\end{aligned}\quad (3.8)$$

and

$$\tilde{\Pi}(\tau, b) = \frac{1}{\tau} e^{2\tilde{A}(\tau, b)} \quad (3.9)$$

The function $2\tilde{A}$ is given by

$$\begin{aligned}2\tilde{A}(\tau, b) &= \tau \int dE e^{-\tau E} \sum_n j \cdot \prod_{i=1}^n \frac{d^3 k_i}{(2\pi)^3 2\epsilon_i} \left| \frac{1}{2s} \tilde{M}(b, k_1, \dots, k_n) \right|^2 \theta(E - \sum \epsilon_i) \\ &= \tau \int dE e^{-\tau E} \left(\frac{E^2}{s} \right)^2 2A(E^2, b) \\ &= \tau \int dE e^{-\tau E} \frac{\mu^2 \beta(0)}{8\pi c s^2 \ln \frac{E^2}{\mu^2}} \left(\frac{E^2}{\mu^2} \right)^{\alpha+1} e^{-\frac{b^2}{4c \ln E^2 / \mu^2}}\end{aligned}\quad (3.10)$$

where α and c are defined as

$$\alpha(k^2) = \alpha(0) - ck^2, \quad \alpha \equiv \alpha(0) \quad (3.11)$$

and we have made use of the structure of $A(s, b)$ given by (2.2). Approximate evaluation yields

$$\tilde{A}(\tau, b) = \frac{\mu^2 \tilde{\beta}}{8\pi c s^2 \ln \frac{1}{\mu^2 \tau^2}} \left(\frac{1}{\tau^2 \mu^2} \right)^{\alpha+1} e^{-\frac{b^2}{4c \ln \frac{1}{\mu^2 \tau^2}}}\quad (3.12)$$

where we have introduced the notation

$$\tilde{\beta} = \Gamma(2\alpha + 3) \beta(0) \quad (3.13)$$

From (3.5), (3.6), and (3.7) we can calculate the inclusive multiparticle distributions, multiplicity and its higher moments, etc. The one-particle inclusive distribution will be worked out to illustrate the technique of Laplace transform and to exhibit its thermodynamic interpretation. The inclusive single particle distribution is given by

$$d\sigma^{(1)}(k) = \int d^2b \frac{L^{-1}[\tilde{\Pi}(\tau, b) \tilde{B}_1(\tau, b, k)]_{E-\epsilon}}{L^{-1}[\tilde{\Pi}(\tau, b)]_E} \frac{d^3k}{\epsilon} \quad (3.14)$$

where

$$\tilde{B}_1(\tau, b, k) = 2\tilde{A}(\tau, b) f(\vec{k}) \quad (3.15)$$

with $f(\vec{k})$ the normalized single particle distribution in the pionization region given by the multiperipheral model.¹⁹ The symbol L^{-1} signifies the inversion of the Laplace transform. The subscripts denote the arguments of the inverse Laplace transforms. The ratio of the inverse Laplace transforms can be easily determined noting that at high energies method of steepest descent is applicable to integrals such as (3.14). Thus

$$d\sigma^{(1)}(k) = \int d^2b \frac{\Pi(E-\epsilon, b)}{\Pi(E, b)} \tilde{B}[\tau(E, b), b, k] \frac{d^3k}{\epsilon} \quad (3.16)$$

with $\tau(E, b)$ determined by the standard relation

$$E = -\frac{\partial}{\partial \tau} 2\tilde{A}(\tau, b) = -\frac{\partial}{\partial \tau} \ln[\tau \tilde{\Pi}(\tau, b)] \quad (3.17)$$

and

$$\frac{\Pi(E-\epsilon, b)}{\Pi(E, b)} = e^{-\tau(E, b)\epsilon} \quad (3.18)$$

Equation (3.17) is recognized to be the familiar connection between the energy E and the partition function $\tilde{\Pi}(\tau, b)$. Equation (3.18) is the well-known Boltzmann factor found in statistical mechanics. The Laplace transform variable τ appears

as the inverse temperature and $\tilde{\Pi}$ the partition function.²⁰ Many physical questions can be answered from thermodynamic considerations.

To demonstrate the method, we now determine the temperature $\tau(E, b)$ for the ϕ^3 ladder exchange. From (3.12) and (3.17), we find

$$\ln \frac{E}{\mu} = (2\alpha+3) \ln \frac{1}{\mu\tau} - \ln \left(\ln \frac{1}{\mu\tau} \right) + \ln \frac{(\alpha+1) \tilde{\beta} \mu^2}{8\pi c s^2} - \frac{b^2}{8c \ln \frac{1}{\mu\tau}} \quad (3.19)$$

For $b^2 \ll \ln^2 \frac{1}{\mu\tau}$, Eq. (3.18) gives

$$\mu\tau(E, b) = \mu\tau(E, 0) \exp \left[- \frac{b^2}{40c \ln \frac{\bar{E}}{\mu}} - 0 \left(\frac{b^2}{\ln^2 \frac{\bar{E}}{\mu}} \right) \right] \quad (3.20)$$

with the definition

$$\mu\tau(E, 0) = \left[\frac{\bar{E}}{\mu} \right]^5 \ln \frac{\bar{E}}{\mu} \quad (3.21)$$

$$\frac{\bar{E}}{\mu} = \left[\frac{40\pi c s^2 E}{(\alpha+1)(2\alpha+3) \tilde{\beta} \mu^3} \right]^{\frac{1}{5}} \propto \frac{\sqrt{s}}{\mu} \quad (3.22)$$

In (3.20) the coefficient of the first correction to the exponent cannot be calculated reliably in our approximation. From the temperature, it is straightforward to determine the remaining quantities. For instance, by substituting (3.20) into (3.12), we obtain

$$\tilde{\Lambda}(\tau(E, b), b) = \frac{(2\alpha+3) \mu^2 \tilde{\beta}}{80\pi c s^2 \ln \frac{\bar{E}}{\mu}} \left[\left(\frac{\bar{E}}{\mu} \right)^5 \ln \frac{\bar{E}}{\mu} \right]^{\frac{2\alpha+2}{2\alpha+3}} \times \exp \left[- \frac{b^2}{40c \ln \frac{\bar{E}}{\mu}} - 0 \left(\frac{b^2}{\ln^2 \frac{\bar{E}}{\mu}} \right) \right] \quad (3.23)$$

Similarly, we can evaluate the one-particle inclusive spectrum,

$$\begin{aligned} d\sigma^{(1)}(k) &= f(\vec{k}) \frac{d^3k}{\epsilon} \frac{(2\alpha+3)\mu^2\tilde{\beta}}{40\pi c s^2 \ln \frac{\bar{E}}{\mu}} \left[\left(\frac{\bar{E}}{\mu} \right)^5 \ln \frac{\bar{E}}{\mu} \right]^{\frac{2\alpha+2}{2\alpha+3}} \\ &\times \int d^2b e^{-\tau(E,b)\epsilon} \exp \left[- \frac{b^2}{40 c \ln \frac{\bar{E}}{\mu}} - 0 \left(\frac{b^2}{\ln^2 \frac{\bar{E}}{\mu}} \right) \right] \end{aligned} \quad (3.24)$$

The b-integration can be carried out, yielding

$$\begin{aligned} d\sigma^{(1)}(k) &= f(\vec{k}) \frac{d^3k}{\epsilon} \frac{(2\alpha+3)\mu^2\tilde{\beta}}{s^2} \left[\left(\frac{\bar{E}}{\mu} \right)^5 \ln \frac{\bar{E}}{\mu} \right]^{\frac{2\alpha+2}{2\alpha+3}} \\ &\times \frac{1}{\tau(E,0)\epsilon} \left(1 - e^{-\tau(E,0)\epsilon} \right) \end{aligned} \quad (3.25)$$

Even though the exact functional form appearing in (3.23) - (3.25) are model dependent, the basic structure of these equations, and in particular, the power E and the exponential b^2 dependences are general features of this class of strong eikonal-Regge model. We shall encounter these basic structures again in Section III. C for another model which is very similar to the vector gluon model.

The two-particle inclusive distributions can also be calculated by similar method. The result is

$$\begin{aligned} d\sigma^{(2)}(k_1, k_2) &= \int d^2b \left[\tilde{B}_2(k_1, k_2) + \tilde{B}_1(k_1) \tilde{B}_1(k_2) \right] e^{-\tau(E,b)(\epsilon_1 + \epsilon_2)} \\ &\times \frac{d^3k_1}{\epsilon_1} \frac{d^3k_2}{\epsilon_2} \end{aligned} \quad (3.26)$$

where

$$\tilde{B}_2(k_1, k_2) = 2\tilde{A}[\tau(E, b), b] f_2(k_1, k_2) \quad (3.27)$$

and $f_2(k_1, k_2)$ is the normalized two-particle inclusive distribution in the multi-peripheral model. The two functions $f(k)$ and $f_2(k_1, k_2)$ are connected when k_1 and k_2 are separated by a large rapidity¹⁹:

$$f_2(k_1, k_2) \rightarrow f(k_1) f(k_2) \quad . \quad (3.28)$$

In (3.26) the term \tilde{B}_2 is the contribution from those events in which both detected particles are emitted from the same ladder, the other term $\tilde{B}_1(k_1) \tilde{B}_1(k_2)$ is the contribution from those events in which both particles are emitted from different ladders.

The b integration in (3.26) can be carried out, and the result is given here for completeness.

$$\begin{aligned} d\sigma^{(2)}(k_1, k_2) &= f_2(k_1, k_2) \frac{d^3k_1}{\epsilon_1} \frac{d^3k_2}{\epsilon_2} \frac{(2\alpha+3)\mu^2\tilde{\beta}}{s^2} \left[\left(\frac{\bar{E}}{\mu} \right)^5 \ln \frac{\bar{E}}{\mu} \right]^{\frac{2\alpha+2}{2\alpha+3}} \\ &\times \frac{1}{\tau(E, 0)(\epsilon_1+\epsilon_2)} \left(1 - e^{-\tau(E, 0)(\epsilon_1+\epsilon_2)} \right), \\ &+ f(k_1) f(k_2) \frac{d^3k_1}{\epsilon_1} \frac{d^3k_2}{\epsilon_2} \frac{(2\alpha+3)^2 \mu^4 \tilde{\beta}^2}{40 \pi c s^4 \ln \frac{\bar{E}}{\mu}} \left[\left(\frac{\bar{E}}{\mu} \right)^5 \ln \frac{\bar{E}}{\mu} \right]^{\frac{4\alpha+4}{2\alpha+3}} \\ &\times \frac{1}{\left[\tau(E, 0)(\epsilon_1+\epsilon_2) \right]^2} \left[1 - e^{-\tau(E, 0)(\epsilon_1+\epsilon_2)} \left(1 + \tau(E, 0)(\epsilon_1+\epsilon_2) \right) \right]. \end{aligned} \quad (3.29)$$

In the central region $\tau(E, 0)(\epsilon_1+\epsilon_2) \ll 1$, and when (3.28) holds (i. e., when particles 1 and 2 are widely separated in rapidity space); (3.29) simplifies to

$$\begin{aligned} d\sigma^{(2)}(k_1, k_2) &= d\sigma^{(1)}(k_1) d\sigma^{(1)}(k_2) \left\{ \frac{1}{80 \pi c \ln \frac{\bar{E}}{\mu}} \right. \\ &\left. + \frac{s^2}{(2\alpha+3) \mu^2 \tilde{\beta}} \left[\left(\frac{\bar{E}}{\mu} \right)^5 \ln \frac{\bar{E}}{\mu} \right]^{-\frac{2\alpha+2}{2\alpha+3}} \right\} . \end{aligned} \quad (3.30)$$

In the strong absorption model, we expect that the picture of short range correlation in the sense of Feynman-Wilson gas analogy no longer holds.

B. Consistency of the Eikonal and the Statistical Models

We now briefly comment on the elastic, inelastic and total cross sections in the strong absorption model. Our purpose is to demonstrate the mutual consistency of the thermodynamic treatment of the inclusive particle distribution properties and the calculation of the cross sections to which no obvious thermodynamic interpretation can be given.

Let's begin with the inelastic cross section. This is given by the sum of (3.5) over N . This sum is demonstrated by large N contributions. When N is large, $\Pi_N(s, b)$ can be obtained by inverting (3.8) for $\tilde{\Pi}_N(\tau, b)$ by the steepest descent method. This gives for large N ,

$$\Pi_N(s, b) = \left[\frac{\text{const}}{\ln \frac{E}{\mu N}} \frac{\left(\frac{E}{\mu N}\right)^{2\alpha+2}}{s^2} e^{-\frac{b^2}{8c \ln \frac{E}{\mu N}}} \right]^N \quad (3.31)$$

As a function of N , $\left[\frac{1}{N!} \Pi_N(s, b) \right]$ is maximum at

$$N = \text{const} \left(\frac{E}{\mu}\right)^{\frac{2\alpha-2}{2\alpha+3}} e^{-\frac{b^2}{40c \ln \frac{E}{\mu}}} \equiv \bar{N}(E, b) \quad (3.32)$$

So approximately we have

$$\Pi_N(s, b) = \text{const} (2 A_{\text{eff}})^N \quad (3.33)$$

with

$$2 A_{\text{eff}} = \frac{\text{const}}{\ln \frac{E}{\mu}} \left(\frac{E}{\mu}\right)^{\frac{2\alpha-2}{2\alpha+3}} e^{-\frac{b^2}{40c \ln \frac{E}{\mu}}} \quad (3.34)$$

It is important to point out that (3.33) is good only for N near \bar{N} , i. e., for $|N - \bar{N}| \ll \bar{N}$. Since $N \sim \bar{N}$ is the region where the dominant contribution arises, this restriction is in fact not important. Notice that both $2A_{\text{eff}}$ and $2\tilde{A}[\tau(E, b), b]$ (see (3.22)) have the same energy dependence. (Recall that $s \sim E^2$.) Substitution of (3.34) into (2.6) gives

$$\sigma_I = \pi b_m^2 \quad , \quad (3.35)$$

$$b_m^2 = \frac{80 c(\alpha-1)}{2\alpha+3} \ln^2 \frac{E}{\mu} \quad . \quad (3.36)$$

This result should be compared with the naive result which follows from (2.7)

$$b_m^2 = 16c(\alpha-1) \ln^2 \frac{E}{\mu} \quad (\text{naive}) \quad . \quad (3.37)$$

The calculation of the elastic amplitude in the strong absorption model is somewhat subtle. This is because the additional constraint required does not follow directly from energy conservation. Rather it arises from the requirement which ensures the validity of the eikonal approximation. According to the analysis of Hasslacher et al.,⁹ in the leading logarithm approximation to the ladder exchanges the eikonal elastic amplitude comes from the contributions of the graphs with the configurations described in Fig. 9, the generalized Mandelstam diagrams.²¹ We will continue to assume this feature to be true in an improved calculation when some nonleading logarithms of the ladder are included. Then in order to ensure that each segment on the top and lower line in Fig. 9 carries practically all the energies of the initial particles, we require

$$\sum \epsilon_i < E = \epsilon \sqrt{s} \quad , \quad 0 < \epsilon \ll 1 \quad ,$$

where the sum extends over all particles in the rungs of all ladders. Here it is understood that the eikonal function is purely absorptive so that all the particles in the rungs are on the mass shell. Then, the contribution to the elastic amplitude

from exchange of N ladders with all possible permutations is

$$T_{E(N)} = 2is \frac{(-1)^N}{N!} \int d^2b e^{i\vec{k} \cdot \vec{b}} \prod_{i=1}^N \sum_N \left| \frac{1}{2s} \tilde{M}(b, k_1^{(i)}, \dots, k_n^{(i)}) \right|^2 \\ \times \theta \left(E - \sum_{\text{all } i} \epsilon_i \right) \prod_{\text{all } j} \frac{d^3 k_j}{(2\pi)^3 2\epsilon_j} \quad (3.38)$$

When N is large the discussion for the inelastic cross section can be repeated here to obtain

$$T_{E(N)} = 2is \frac{(-1)^N}{N!} \int d^2b e^{i\vec{k} \cdot \vec{b}} (A_{\text{eff}})^N \quad (3.39)$$

with A_{eff} given by (3.34). Thus, the eikonal function which appears in the elastic amplitude and that in the inelastic cross section agree.

In retrospect, we can construct an eikonal model in the strong absorption for the elastic amplitude and inelastic cross sections by retaining the naive results such as (3.1) and (3.2) but change the upper limit of integrations (3.3) to

$$\mu \leq \epsilon_i < \frac{E}{N} = \mu \left(\frac{E}{\mu} \right)^{\frac{5}{2\alpha+3}} e^{-\frac{b^2}{40c \ln \frac{E}{\mu}}} \quad (3.40)$$

where N is given by (3.32). Obviously this construction yields all the correct results. It is interesting that the upper limit (3.40) depends on the impact parameter. Apart from the impact-parameter dependent factor, (3.40) is precisely the prescription given in Ref. 6 to correct for the energy loss. Here, it emerges as a result of taking into account the necessary constraints to ensure the validity of the eikonal approximation.

Unitarity relates the virtual processes which determine the elastic amplitude and the real production processes. It is satisfying to know that our treatments of both virtual and real processes are mutually consistent.

C. Weak Pomeron Model

Finally, we sketch briefly the analogy as well as some quantitative changes if the Regge pole has an intercept which starts out from 1. We call this the weak Pomeron model. Apart from some minor differences this model shares many similar properties with the vector gluon model studied extensively by Chang and Wu. As one can verify readily, all the general conclusions of the theory, such as described in (3.5), (3.7) - (3.9), (3.14) - (3.18) and (3.26) - (3.28), etc., are not modified. However, the quantitative expressions of the potential $A(s, b)$, the temperature function $\tau(E, b)$, the multiplicity distribution $N(E, b)$, and the one- and two-particle spectra are somewhat different. We list in the following the corresponding expressions in the weak Pomeron model for completeness: (These equations are the analog of (3.10), (3.20), (3.23), (3.25), and (3.29) respectively.).

$$\begin{aligned} \tilde{A}(\tau, b) &\equiv \int dE e^{-\tau E} A(E, b) \\ &= \frac{\tilde{\beta}}{16\pi c\mu^2 \ln \frac{1}{\mu\tau}} \left(\frac{1}{\mu\tau}\right)^{2\alpha-2} e^{-\frac{b^2}{8c \ln \frac{1}{\mu\tau}}} ; \end{aligned} \quad (3.41)$$

$$\mu\tau(E, b) = \mu\tau(E, 0) \exp\left(-\frac{b^2}{8c \ln \frac{\bar{E}}{\mu}}\right) ,$$

$$\mu\tau(E, 0) = \left(\frac{\bar{E}}{\mu} \ln \frac{\bar{E}}{\mu}\right)^{-\frac{1}{2\alpha-1}} ,$$

$$\bar{E} \equiv \frac{8\pi c\mu^2 E}{(2\alpha-1)(\alpha-1)\tilde{\beta}} ; \quad (3.42)$$

$$\begin{aligned}
N(\mathbf{E}, b) = \tilde{A}(\tau(\mathbf{E}, b), b) &= \frac{(2\alpha-1)\bar{\beta}}{16\pi c\mu^2} \frac{\left(\frac{\bar{E}}{\mu} \ln \frac{\bar{E}}{\mu}\right)^{\frac{2\alpha-2}{2\alpha-1}}}{\ln \frac{\bar{E}}{\mu}} \\
&\times \exp\left(-\frac{b^2}{8c \ln \frac{\bar{E}}{\mu}}\right) ; \tag{3.43}
\end{aligned}$$

$$d\sigma^{(1)}(\mathbf{k}) = f(\vec{k}) \frac{d^3k}{\epsilon} \frac{(2\alpha-1)\bar{\beta}}{\mu^2} \left(\frac{\bar{E}}{\mu} \ln \frac{\bar{E}}{\mu}\right)^{\frac{2\alpha-2}{2\alpha-1}} \frac{1 - e^{-\tau(\mathbf{E}, 0)\epsilon}}{\tau(\mathbf{E}, 0)\epsilon} \tag{3.44}$$

and

$$\begin{aligned}
d\sigma^{(2)}(\mathbf{k}_1, \mathbf{k}_2) &= f_2(\mathbf{k}_1, \mathbf{k}_2) \frac{d^3k_1}{\epsilon_1} \frac{d^3k_2}{\epsilon_2} \frac{(2\alpha-1)\bar{\beta}}{\mu^2} \left(\frac{\bar{E}}{\mu} \ln \frac{\bar{E}}{\mu}\right)^{\frac{2\alpha-2}{2\alpha-1}} \\
&\times \frac{1 - e^{-\tau(\mathbf{E}, 0)(\epsilon_1 + \epsilon_2)}}{\tau(\mathbf{E}, 0)(\epsilon_1 + \epsilon_2)} \\
&+ f(\mathbf{k}_1) f(\mathbf{k}_2) \frac{d^3k_1}{\epsilon_1} \frac{d^3k_2}{\epsilon_2} \frac{(2\alpha-1)^2 \bar{\beta}^2}{8\pi c\mu^4} \left(\frac{\bar{E}}{\mu} \ln \frac{\bar{E}}{\mu}\right)^{\frac{4\alpha-4}{2\alpha-1}} \\
&\times \frac{1 - e^{-\tau(\mathbf{E}, 0)(\epsilon_1 + \epsilon_2)} \left[1 + \tau(\mathbf{E}, 0)(\epsilon_1 + \epsilon_2)\right]}{\left[\tau(\mathbf{E}, 0)(\epsilon_1 + \epsilon_2)\right]^2} . \tag{3.45}
\end{aligned}$$

Interested readers are invited to reproduce these expression for an exercise.

The result (3.44) for the vector gluon model in the region $\tau(\mathbf{E}, 0)\epsilon \ll 1$ has been obtained by Cheng and Wu. ²²

IV. RESULTS AND IMPLICATIONS

In this section, we present the main results obtained in the present paper and discuss their implications. We shall concentrate on the general features of the results which appear in both the ϕ^3 and the weak Pomeron model (WPM), and shall emphasize on the possible physical and geometrical interpretation.

A. Width and Height of the Central Plateau

From (3.24) and (3.44), it is seen that the one-particle inclusive cross section in the central region for a fixed impact parameter b has the general structure (to within $\ln E$ -factor),

$$d\sigma^{(1)} \propto f(k_{\perp}) \frac{d^3k}{\epsilon} E^a e^{-\tau(E,b)\epsilon} e^{-\frac{b^2}{c_1 Y_0}} \quad (4.1)$$

with

$$\frac{1}{\tau(E,b)} \propto E^{1-a} e^{\frac{b^2}{c_1 Y_0}} \quad (4.2)$$

where Y_0 is the magnitude of the rapidity of the incident particles,

$$Y_0 = \ln E/\mu \quad . \quad (4.3)$$

Parameter \underline{a} controls the energy dependent height of the central plateau, and c_1 is related to the expanding rate of the absorption disc. These parameters are measurable quantities, and will appear frequently in our discussion. In ϕ^3 and WPM, they are given respectively as

$$\begin{aligned} a &= \frac{2(\alpha-1)}{2\alpha+3} && (\phi^3 \text{ theory}) \\ &= \frac{2(\alpha-1)}{2\alpha-1} && (\text{WPM}) \end{aligned} \quad (4.4)$$

and

$$\begin{aligned} c_1 &= 40 c && (\phi^3 \text{ theory}) \\ &= 8 c && (\text{WPM}) \end{aligned} \quad (4.5)$$

Note that $0 < a < 1$ in the strong coupling case and $a \rightarrow 0$ as $\alpha \rightarrow 1$.

From (4.1), we find that the central plateau has a b -dependent width,

$$D(b) = \ln \frac{1}{\tau(E, b)} = (1-a) Y_0 + \frac{b^2}{c_1 Y_0} + o(1) \quad , \quad (4.6)$$

and a b -dependent height,

$$H(b) = e^{aY_0} e^{-\frac{b^2}{c_1 Y_0}} \quad . \quad (4.7)$$

The width $D(b)$ and the height $H(b)$ are related by

$$D(b) + \ln H(b) = Y_0 \quad (4.8)$$

independent of the parameter a and the impact parameter b . The width $D(b)$ increases as b increases, while the height $H(b)$ has the opposite effect. When integrated over all values of b , the final single particle distribution (3.25) or (3.44) gives a flat central plateau of width

$$D = \ln \frac{1}{\tau(E, 0)} = (1-a) Y_0$$

and a height

$$H = e^{aY_0} \quad .$$

We observe that the width on the rapidity axis occupied by the pionization particles does not cover the whole available region $2Y_0$. There exists a rapidity gap $\Delta(Y)$

$$\frac{1}{2} \Delta(Y) = aY_0 \quad . \quad (4.11)$$

This gap is related to the increase of plateau height at increasing E , and is required by energy conservation when the multiplicity is a power of energy.

B. Energy and Multiplicity Sum Rules

The consistency of (3.25) and (3.44) for $d\sigma^{(1)}(k)$ can be checked by the energy conservation sum rule

$$\int \epsilon d\sigma^{(1)}(k) = E\sigma_T \quad . \quad (4.12)$$

Explicit evaluation of the integral gives

$$\int \epsilon d\sigma^{(1)}(k) = \text{const } (\alpha-1) \left[\int d^2\vec{k} f(\vec{k}) \right] \frac{E}{\mu} \ln^2 \frac{E}{\mu} \quad . \quad (4.13)$$

The constant in the front of (4.13) can be computed exactly, and is found to depend on large $b(\sim \ln E)$ integration region. Since the thermodynamics approximation breaks down in this kinematical region, the constant computed from (3.25) and (3.44), which follow from the thermodynamics treatment, is no longer reliable. Nevertheless, (4.13) gives the correct energy dependence and it is consistent with the energy dependence of σ_T given by

$$\sigma_T = 2\pi c_1 a \ln^2 E \quad (4.14)$$

From (3.24) or (3.44) we can also calculate the average multiplicity $\langle n \rangle$ from the sum rule

$$\int d\sigma^{(1)}(k) = \langle n \rangle \sigma_I \quad (4.15)$$

We find,²³

$$\langle n \rangle \sigma_I = \text{const} \int d^3\vec{k} f(\vec{k}) \frac{\left(\frac{E}{\mu}\right)^a}{\left(\ln \frac{E}{\mu}\right)^{c_2}} \left(\ln \frac{E}{\mu}\right)^2 \quad , \quad (4.16)$$

with

$$c_2 = a/2(\alpha-1) \quad . \quad (4.17)$$

Since²⁴

$$\sigma_I = \text{const} + \pi c_1 a \ln^2 \frac{E}{\mu}, \quad (4.18)$$

the average $\langle n \rangle$ grows as a power of total c. m. energy within logarithmic corrections

$$\langle n \rangle = \text{const} \frac{\left(\frac{E}{\mu}\right)^a}{\left(\ln \frac{E}{\mu}\right)^{c_2}}. \quad (4.19)$$

A careful examination of the b -integral reveals that the important region of b extends to $b^2 \sim \ln^2 E$ for the energy conservation sum rule (4.12); on the other hand, the contribution to $\langle n \rangle$ is dominated by $b^2 \lesssim \ln E$. This indicates that most of the particles are produced in the region of small b with low energies. This is the reason why the temperature $\frac{1}{\tau(E, b)}$ is lowest at $b=0$, according to (3.20) and (3.42).

C. Moments of Multiplicity and Particle Sizes

As another application of our results we calculate the second moment of the multiplicity given by

$$\begin{aligned} \int d\sigma^{(2)}(k_1, k_2) &= \langle n(n-1) \rangle \sigma_I \\ &= \langle n \rangle^2 \sigma_I^2 \left[\frac{1}{2\pi c_1 \ln \frac{E}{\mu}} + \text{const} \left(\frac{E}{\mu}\right)^{-a} \left(\ln \frac{E}{\mu}\right)^{-1+c_2} \right] \end{aligned} \quad (4.20)$$

Hence

$$\begin{aligned} \frac{\sigma_I \int d\sigma^{(2)}(k_1, k_2)}{\left[\int d\sigma^{(1)}(k) \right]^2} &= \frac{\langle n(n-1) \rangle}{\langle n \rangle^2} \\ &= \frac{\sigma_I}{2\pi c_1 \ln \frac{E}{\mu}} (1+R) \end{aligned} \quad (4.21)$$

where $R \rightarrow 0$ as $E \rightarrow \infty$. Thus

$$\frac{\langle n(n-1) \rangle}{\langle n \rangle^2} \sim \ln \frac{E}{\mu} \quad (4.22)$$

This result differs from that in the multiperipheral model in which the right-hand side is a constant.²⁵

To understand (4.21), (4.22) qualitatively, we recall that there are two relevant sizes or radii of the particle in our problem. This can be seen most easily from the multiplicity distribution function N in (3.32) or (3.43),

$$N(E, b) \propto E^a e^{-\frac{b^2}{c_1 \ln \frac{E}{\mu}}} \quad (4.23)$$

The radius b_m which determines the total elastic and inelastic cross sections is given by $N \approx 1$, and has the value (see Eq. (3.36))

$$b_m^2 = c_1 a \ln^2 \frac{E}{\mu} \quad (4.24)$$

However, for the multiplicity is concerned, the dominant contribution comes from a smaller radius b_s characterized by the width of the gaussian distribution (see Fig. 10),

$$b_s^2 \approx c_1 \ln \frac{E}{\mu} \ll b_m^2 \quad (4.25)$$

To the first approximation, we can replace $N(E, b)$ in (4.23) by

$$N(E, b) = N(E, 0) \theta(b_s^2 - b^2) \quad (4.26)$$

It is also known that the multiladder emission in b -space in our model is approximately independent, and hence, the multiplicity distribution in b -space is essentially Poisson,

$$n^2(b) - n(b) \approx (n(b))^2 \quad (4.27)$$

Integrating $n(b)$ and $n^2(b) - n(b)$ over b , we have

$$\sigma_I \langle n \rangle = \int d^2b n(b) \approx n(0) \pi b_s^2 \quad (4.28)$$

$$\sigma_I \langle n^2 - n \rangle = \int d^2b (n(b))^2 \approx (n(0))^2 \pi b_s^2 \quad (4.29)$$

Hence, we have

$$\frac{\langle n^2 - n \rangle}{\langle n \rangle^2} \approx \frac{\sigma_I}{\pi b_s^2} \propto \frac{\sigma_I}{\ln E/\mu} \quad (4.30)$$

as desired. In other words, the mismatch of radii in (4.24) and (4.25) is crucial for the arriving of results (4.21) and (4.22). Equation (4.22) is valid only in the extremely high energy. At the present energy range, σ_I only increases slightly with E and thus the left-hand side of (4.21) may not increase notably at all. Thus, the so-called KND scaling may be approximately valid at the present energy.²⁵

D. Effects of Fragmentation and Many-Body Potentials

We will now briefly summarize the effects of including the fragmentation and many-body potentials on the results presented above. We will ignore the momentum transfer dependences in the "wave functions" so that the various cross sections can be expressed by a single impact parameter representation. We will also assume that the exchanged object is a t -channel ladder. Thus, we have included up to four-body potentials.

1. Central region

Only the fragmentation of particle a will be considered to simplify the discussion. In the notation of (2.65) the one- and two-particle inclusive cross

sections in the central region are

$$d\sigma^{(1)}(k) = \left[c + \sum_{N=2}^{\infty} N^2 \int d\mathbb{I}_N^{(a)}(1, 2, \dots, N) \right] \left[d\sigma^{(1)}(k) \right]_{B_1} \quad (4.31)$$

$$\begin{aligned} d\sigma^{(2)}(k_1, k_2) &= \left[c + \sum_{N=2}^{\infty} N^2 \int d\mathbb{I}_N^{(a)}(1, 2, \dots, N) \right] \left[d\sigma^{(2)}(k_1, k_2) \right]_{B_2} \\ &+ \left\{ \sum_{N=2}^{\infty} N(N-1) \int d\mathbb{I}_N^{(a)}(1, 2, \dots, N) \right\} \left[d\sigma^{(2)}(k_1, k_2) \right]_{B_1 B_1} \end{aligned} \quad (4.32)$$

where we have employed the notations

$$\left[d\sigma^{(1)}(k) \right]_{B_1} = \int d^2b \tilde{B}_1[\tau(E, b), b, k] e^{-\tau(E, b)\epsilon} \frac{d^3k}{\epsilon} \quad , \quad (4.33)$$

$$\left[d\sigma^{(2)}(k_1, k_2) \right]_{B_2} = \int d^2b \tilde{B}_2(k_1, k_2) e^{-\tau(E, b)(\epsilon_1 + \epsilon_2)} \frac{d^3k_1}{\epsilon_1} \frac{d^3k_2}{\epsilon_2} \quad , \quad (4.34)$$

$$\left[d\sigma^{(2)}(k_1, k_2) \right]_{B_1 B_1} = \int d^2b \tilde{B}_1(k_1) \tilde{B}_1(k_2) e^{-\tau(E, b)(\epsilon_1 + \epsilon_2)} \frac{d^3k_1}{\epsilon_1} \frac{d^3k_2}{\epsilon_2} \quad (4.35)$$

and B_1 and B_2 are given by (3.15) and (3.27).

From (4.31) we see that fragmentation and many-body potentials only change the overall energy independent normalization of the one-particle inclusive cross section, and hence the average multiplicity. This is not true for the two-particle and n -particle ($n \geq 2$) inclusive distributions. The two detected particles may come from a single ladder attached to different fragments or they may come from different ladders attached to different fragments. These possibilities are represented respectively by the first and the second series in (4.32). Although the two particles coming from a single ladder do exhibit the short range correlation in rapidity,²⁶ this contribution is nonleading. Because of the existence

of many competing mechanisms there seems no obvious and physically meaningful way to define the two-particle correlation. The normalization is complicated and no obvious definition seems to provide any interesting information.

2. Fragmentation region

We have also calculated the one-particle inclusive distribution in the fragmentation region. It is

$$\epsilon_1 \frac{d\sigma}{d^3k_1} = (\pi b_m^2) \left[\sum_{N=2}^{\infty} N \int d(2) d(3) \dots dN |\psi_a(1, 2, \dots, N)|^2 \right] \quad (4.36)$$

where

$$d(1) d(2) \dots dN |\psi_a(1, 2, \dots, N)|^2 = dI_N^{(a)}(1, 2, \dots, N) \quad (4.37)$$

and $d(1) d(2) \dots dN$ is the phase-space volume element. Equation (4.36) exhibits the Feynman's scaling²⁷ or Benecke, Chou, Yang and Yen's limiting distribution²⁸ for the combination $\frac{1}{\sigma_T} \epsilon_1 \frac{d\sigma}{d^3k_1}$. This is in contrast to the one-particle inclusive cross section (4.31) where the scaling behavior is violated.

It is clear that there is no physical correlation between a left-moving and a right-moving fragment, in the sense that

$$\frac{1}{\sigma_T} \epsilon_L \epsilon_R \frac{d\sigma^{(2)}}{d^3k_L d^3k_R} = \text{const} \left[\frac{1}{\sigma_T} \epsilon_L \frac{d\sigma^{(1)}}{d^3k_L} \right] \left[\frac{1}{\sigma_T} \epsilon_R \frac{d\sigma^{(1)}}{d^3k_R} \right] \quad (4.38)$$

Of course, there is a strong correlation between two right- (left-) moving fragments. For example, for two fragments of particle a, we find

$$\epsilon_1 \epsilon_2 \frac{d\sigma^{(2)}}{d^3k_1 d^3k_2} = (\pi b_m^2) \sum_{N=2}^{\infty} N(N-1) \int d(3) d(4) \dots dN |\psi_a(1, 2, 3, \dots, N)|^2 \quad (4.39)$$

3. Ratio of elastic to total cross section

An important consequence of including the fragmentation events in the strong absorption is that the ratio of the elastic to the total cross section is no longer one half. This ratio is reduced from $1/2$ since the incident particles have only fractional relative probabilities to maintain their identities. It is only the sum of the elastic and diffractive cross sections that remains to be $1/2$ of the total cross section.

V. DISCUSSIONS

We have presented in some detail the results of a eikonal model with rising cross sections. Whether such a model represents the truth of the real world is not clear. Although, as mentioned in the introduction, there are some encouraging signs from the recent ISR data, there are also some possible difficulties. Among them we mention the rapidity gap between the pionization region and the fragmentation region, a feature has not yet been observed experimentally. Perhaps the gap exists only because we have not handled the fragmentation properly. Clearly if a smooth transition is to occur between the fragmentation and the pionization region, there must be some stringent conditions on the eikonal function and the fragmentation amplitudes. Most likely the energy dependence of the eikonal function will be weakened and at the same time fragmentation states with higher masses should be incorporated.¹⁶ We are not able to see how the smoothness may be achieved if the total cross section is to increase as $\ln^2 E$ with the energy.

Another difficult question concerns the validity of keeping only the ladder exchanges in the field theories. Many authors have issued the warning,²⁹ based on some model studies, that when all exchanged connected pieces are summed, the eikonal function may have an energy dependence very different from individual terms. The starting point of the present paper is the premise that the total cross sections saturate the Froissant bound. The model studied in this paper is the simplest one to realize this possibility. Presumably this question is also related to the t-channel unitarity. We have no idea how much of our results will be modified when the t-channel unitarity is enforced.

We became aware of two very interesting pieces of work when this paper was in preparation: (1) Sugar³⁰ recently has studied the effect of the isospin

in the eikonal-Regge type model. He assumed that both the sides (called ρ) and the rungs (called π) of a t-channel ladder carry unit isospin, and that the pions are coupled to the isospin current of the ρ 's. In this model, Sugar demonstrated at high energy that the pion cannot be emitted from a ladder, and its emission amplitude is dampened dynamically by a power of s . Hence, any t-channel exchange more complicated than a ladder is suppressed dynamically because it involves the emission and absorption of π 's from ladders. Thus, one is led automatically to the elastic and the inelastic contributions as given in Figs. 1 and 2. (2) Steinhoff³¹ has examined the asymptotic behavior of the elastic and the one-particle inclusive spectrum in the ϕ^3 ladder amplitude by means of statistical mechanics method. He found that the transverse momentum dependence in $d\sigma^{(1)}$ is given by

$$f(k_{\perp}) \propto e^{-\text{const} \sqrt{k_{\perp}^2 + \mu^2}} .$$

Steinhoff also demonstrated that the above result is also valid in the generalized ladder amplitude with the rungs being crossed in all possible ways. It should be pointed out that the above result is valid in the dual model as well. On the other hand, the above $f(k_{\perp})$ is completely different from those obtained in the straight ladder amplitude based on the leading logarithm approximation where only the correlation between nearest rungs are included,

$$f(k_{\perp})_{\text{leading log}} \propto \frac{1}{(k_{\perp}^2 + m^2)^2} .$$

Thus, the exponential damping in $f(k_{\perp})$ probably reflects the many-body correlation effects, and is insensitive to the detailed dynamics. It would be interesting to know which and how many of the observed hadron phenomena can be understood easily in terms of the statistical mechanics language.

Acknowledgements

One of us (SJC) wishes to thank Professors K. Gottfried and E. Berger for many stimulating discussions. One of us (TMY) wishes to thank Aspen Center for Physics and Professor S. D. Drell of SLAC respectively for the hospitality during the summer of 1973 and the year 1973-74.

FOOTNOTES AND REFERENCES

1. For an assessment of the present theoretical understanding of the eikonal approach to high energy hadron scatterings, see the excellent article by R. Blankenbecler, J. R. Fulco and R. L. Sugar, Report No. SLAC-PUB-1281, Stanford Linear Accelerator Center (1973). For important references on this subject the reader is invited to consult this paper.
2. U. Amaldi et al., Phys. Letters 44B, 112 (1973);
S. R. Amendolia et al., Phys. Letters 44B, 119 (1973).
3. H.D.I. Abarbanel and C. I. Itzykson, Phys. Rev. Letters 23, 53 (1969);
B. M. Barbashov et al., Teor. Mat. Fiz. 3, 342 (1970).
4. M. Levy and J. Sucher, Phys. Rev. 186, 1656 (1969);
F. Englert et al., Nuovo Cimento 64A, 561 (1969).
5. R. Blankenbecler and R. Sugar, Phys. Rev. D 2, 3024 (1970).
6. S. J. Chang and T. M. Yan, Phys. Rev. Letters 25, 1586 (1970);
Phys. Rev. D 4, 537 (1971).
7. B. Hasslacher et al., Phys. Rev. Letters 25, 1891 (1970).
8. G. M. Cicuta and R. L. Sugar, Phys. Rev. D 3, 970 (1971).
9. B. Hasslacher and D. K. Sinclair, Phys. Rev. D 3, 1770 (1971).
10. S. J. Chang and S. Ma, Phys. Rev. Letters 22, 1334 (1969);
Phys. Rev. 188, 2385 (1969).

11. S. J. Chang and P. M. Fishbane, Phys. Rev. D 2, 1104 (1970);
Phys. Rev. D 3, 1047 (1971).
12. H. Cheng and T. T. Wu, Phys. Rev. 186, 1611 (1969).
13. H. Cheng and T. T. Wu, Phys. Rev. Letters 24, 1456 (1970), and
references cited therein.
14. G. Calucci, R. Jengo and C. Rebbi, Nuovo Cimento 4A, 330 (1971),
Nuovo Cimento 6A, 601 (1971); R. Aviv, R. Blankenbecler and R. Sugar,
Phys. Rev. D 5, 3252 (1972); S. Auerbach, R. Aviv, R. Blankenbecler,
and R. Sugar, Phys. Rev. Letters 29, 522 (1972), Phys. Rev. D 6,
2216 (1972); R. Sugar, Phys. Rev. D (to be published); S. Auerbach,
U. C. Berkeley preprint.
15. A preliminary account of the results of this paper appear in S. J. Chang
and T. M. Yan, Report No. SLAC-PUB-1381, Stanford Linear Accelerator
Center (1974).
16. J. Skard and J. R. Fulco, Phys. Rev. D 8, 312 (1973). These authors
and those of Ref. 1 assume that the fragmentation states can be effectively
described by a single impact parameter.
17. The method used in the following discussion is a generalization of that used
in Ref. 6.
18. This is not true in the massive vector gluon model since the electron and
the positron have opposite charge.
19. For a discussion of the functions $f(k)$ and $f(k_1, k_2)$ [Eq. (3.27)] in the ϕ^3
multiperipheral model, see, for example, S. J. Chang, T. M. Yan, and
Y. P. Yao, Phys. Rev. D 4, 3012 (1971).
20. Unlike the mathematical analogy between the particle distributions in
rapidities in the multiperipheral model and a one-dimensional gas

system, the thermodynamic interpretations of τ and Π are physically meaningful.

21. B. Hasslacher and D. K. Sinclair, Ref. 9. In the case of two-ladder exchange, this statement has been explicitly verified, see Refs. 7, 8 and 9.
22. H. Cheng and T. T. Wu, Phys. Letters 45B, 367 (1973).
23. The numerical coefficient for $\langle n \rangle$ is proportional to $g^2 \frac{d\alpha}{dg^2}$. Thus, if $\alpha-1$ is to be small as suggested by the data, $g^2 \frac{d\alpha}{dg^2}$ is expected to be small in the massive vector gluon model since the coupling must be weak. This need not be the case in the ϕ^3 theory in which α exceeds unity only when the coupling is sufficiently strong. See T. Goldman and D. Sivers, Phys. Letters 48B, 39 (1974).
24. In (4.18) we have added the constant term which does not vanish in the limit $\alpha \rightarrow 1$.
25. Equation (4.22) shows that the so-called KNO scaling is violated asymptotically in this model. Koba, Nielsen and Oleesen, Nucl. Phys. B40, 317 (1972). See also H. M. Fried and C. I. Tan, Phys. Rev. D 9, 314 (1974).
26. K. Wilson, Cornell Report 131 (1970); A. Mueller, Phys. Rev. D 4, 150 (1971); D. K. Campbell and S. J. Chang, Phys. Rev. D 4, 1151 (1971); S. J. Chang, T. M. Yan, and Y. P. Yao, Phys. Rev. D 4, 3012 (1971); T. D. Lee, Phys. Rev. D 6, 3617 (1972).
27. R. P. Feynman, Phys. Rev. Letters 23, 1415 (1969).
28. J. Benecke, T. T. Chou, C. N. Yang, and E. Yen, Phys. Rev. 188, 2159 (1969).

29. S. Auerbach, R. Aviv, R. Blankenbecler, and R. Sugar, Ref. 14;
R. Sugar, Ref. 14; R. Blankenbecler and H. Fried, Phys. Rev. D 8,
678 (1973).
30. R. Sugar, private communication.
31. J. Steinhoff, "Multiperipheral models: A self-consistent field approach,"
McGill preprint (1974).

FIGURE CAPTIONS

1. The elastic amplitude studied in this paper. The lines labelled a_1, \dots, a_n (b_1, \dots, b_m) represent the fragments of particle a (particle b). The blobs exchanged between a and b are t-channel ladders.
2. A typical inelastic amplitude studied in this paper.
3. Example of elastic amplitudes with two fragments in particle a and no fragmentation in particle b. The ladders link all 3 lines.
4. Same as Fig. 3 except that the ladder only links one fragment of a to particle b.
5. Elastic amplitude with three fragments in particle a and no fragmentation in particle b.
6. Elastic amplitude with two fragments each in particle a and b.
7. Ladder-exchange which leads to four-body eikonal function (i.e., four-body potential).
8. Production processes associated with Figs. 3 and 4.
9. The generalized Mandelstam diagrams, also known as the "nested diagrams," studied in Ref. 9.
10. (a) Multiplicity distribution in b-space;
(b) Two relevant radii b_s (half-width) and b_m (maximal size) obtained from the distribution curve.

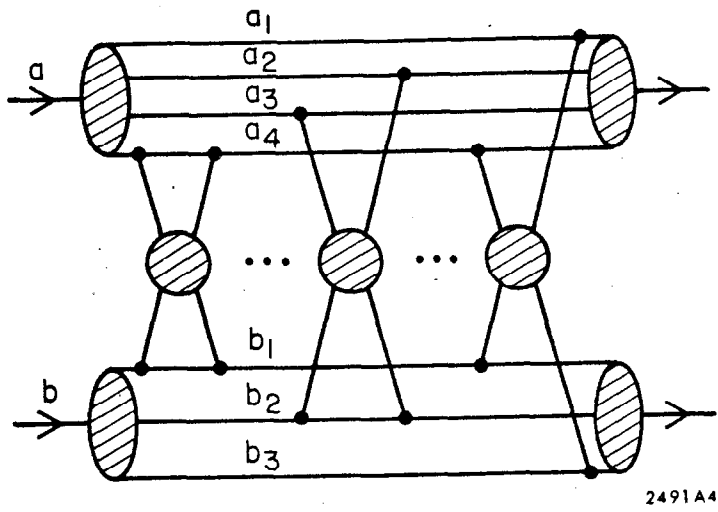


Fig. 1

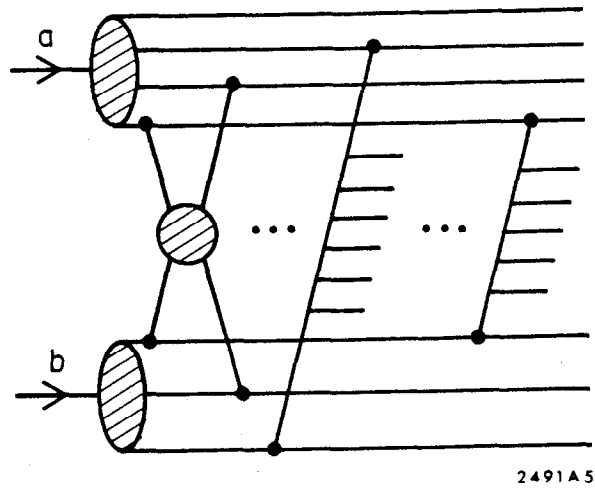


Fig. 2

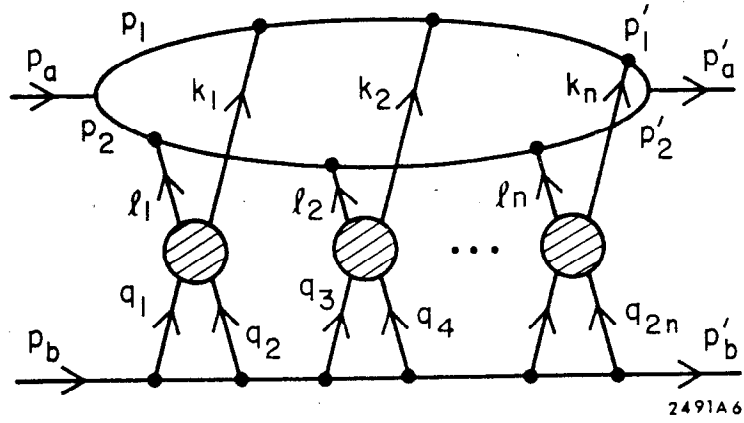


Fig. 3

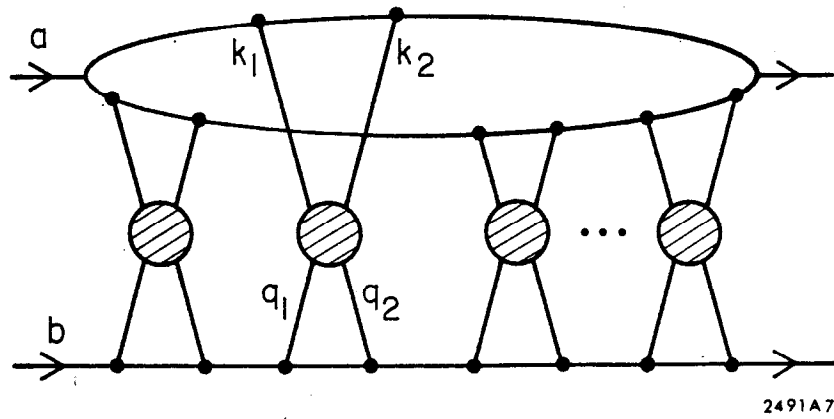


Fig. 4

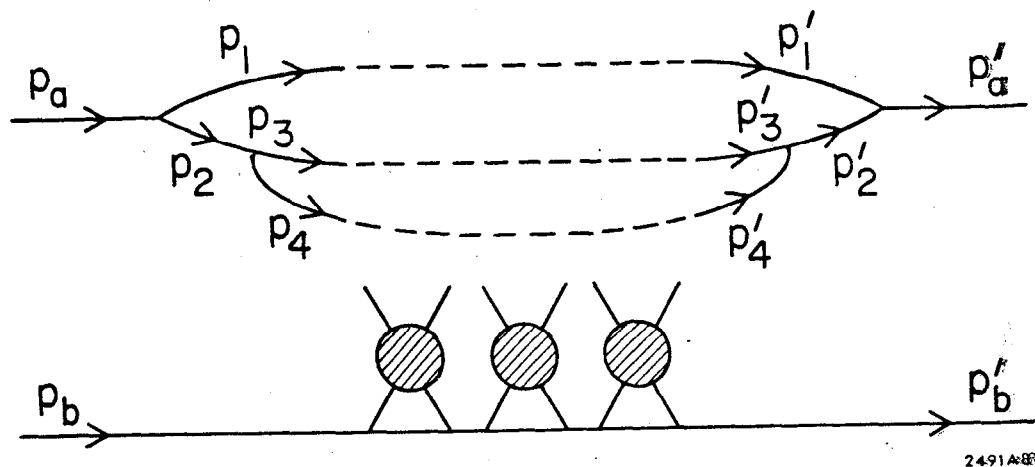


Fig. 5

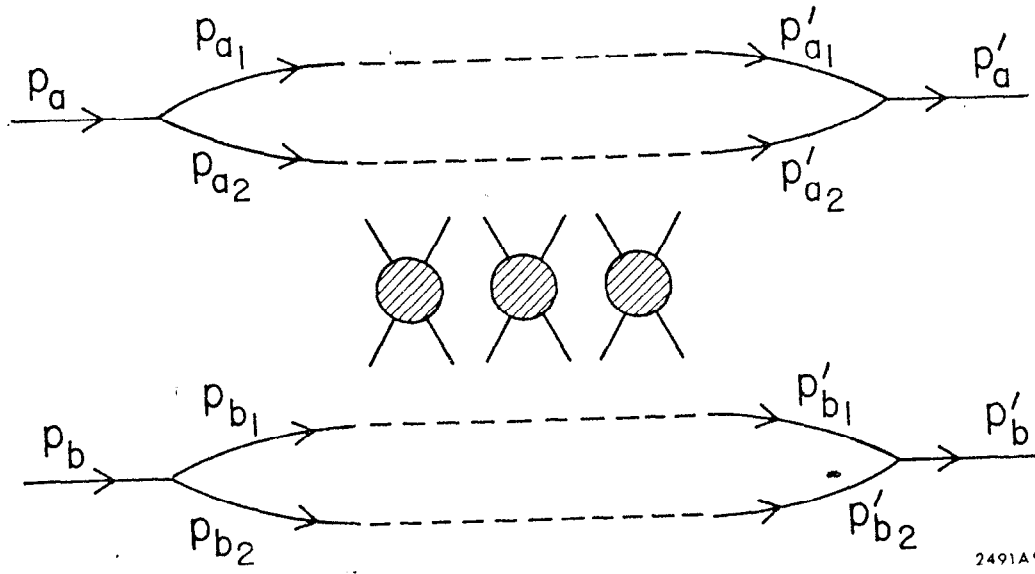


Fig. 6

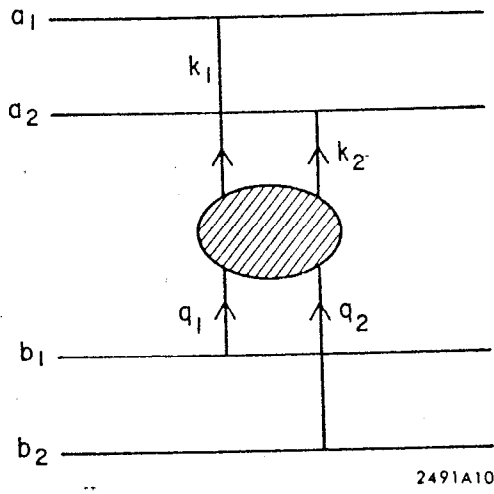


Fig. 7

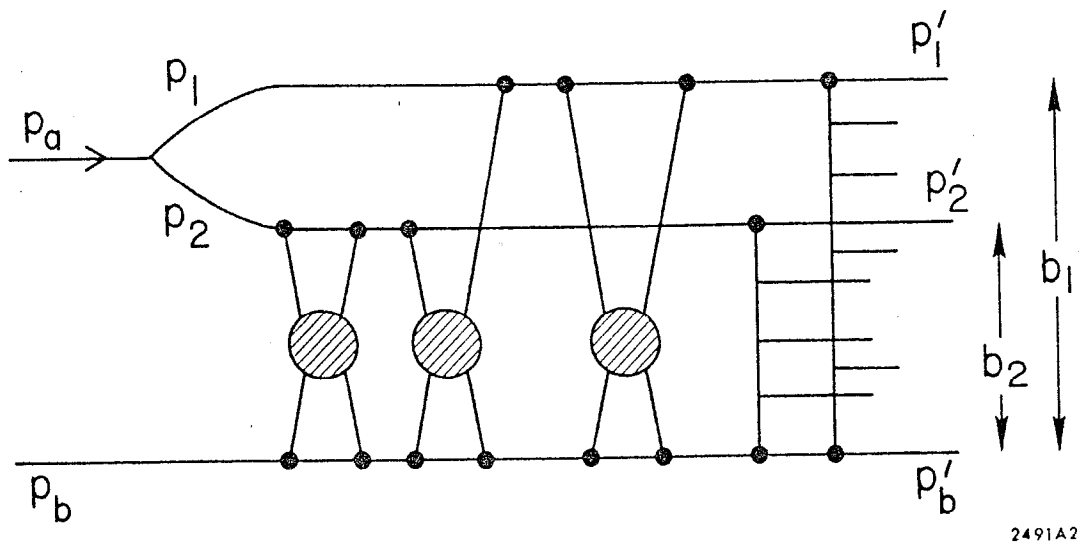
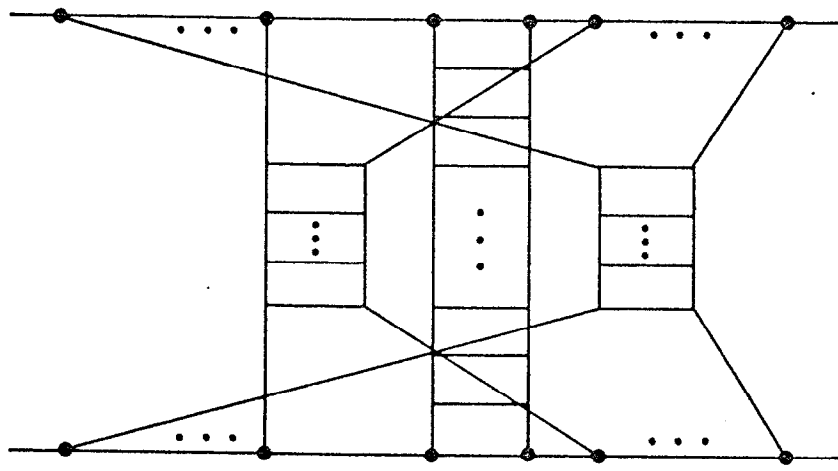
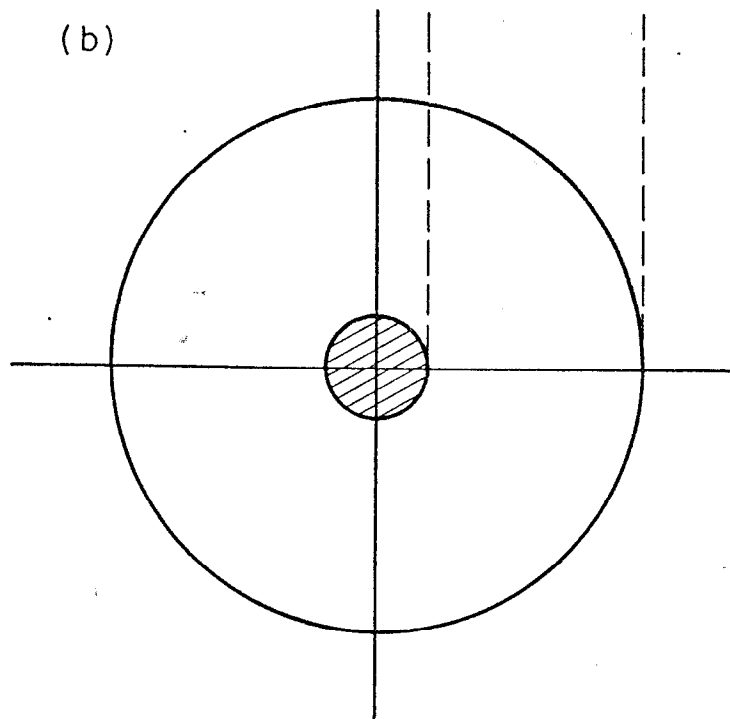
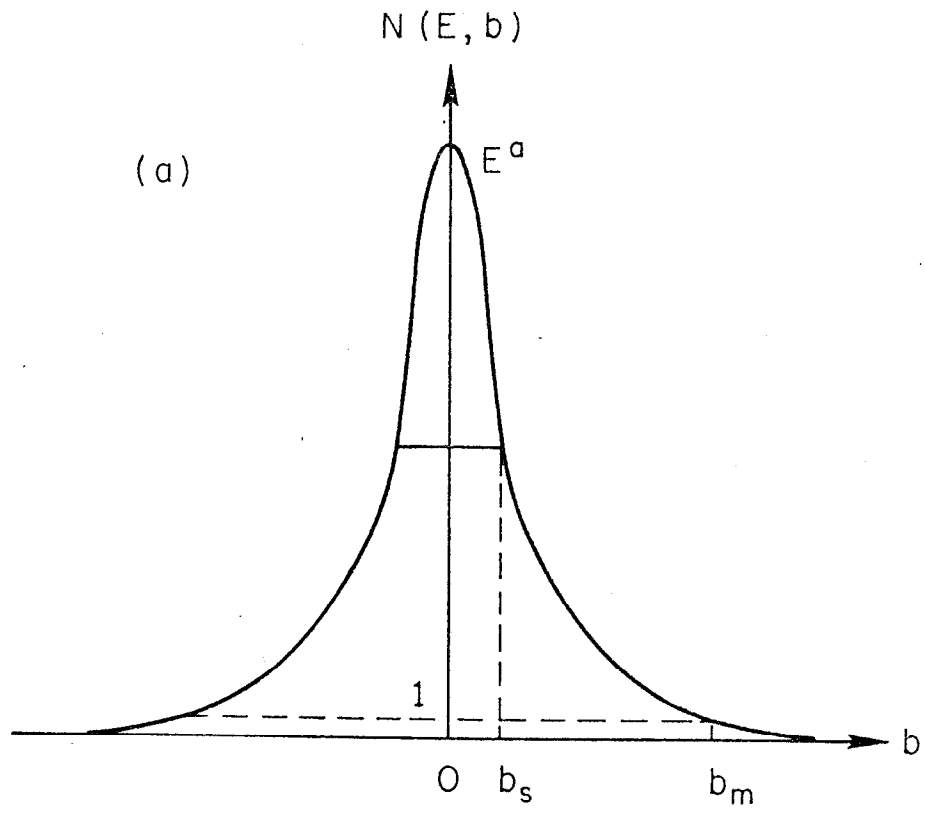


Fig. 8



2491A3

Fig. 9



2491A1

Fig. 10